universität wien

DISSERTATION

Titel der Dissertation

CALCIUM CHANNEL BLOCK BY DILTIAZEM

Verfasser

Waheed Shabbir BSc (hons), Msc

angestrebter akademischer Grad

Doktor der Naturwissenschaften (Dr.rer.nat.)

Wien, 2011

Studienkennzahl lt. Studienblatt:	A 091 490
Dissertationsgebiet lt. Studienblatt:	Molekulare Biologie
Betreuerin / Betreuer:	Univ.Prof. Dr. Steffen Hering

Abbreviations

VDCC	Voltage-dependent calcium channels
Ca_V	Voltage-gated calcium channel
HEK	Human embryonic kidney cells
BTZ	Benzothiazepines
DHP	Dihydropyridines
PAA	Phenylalkylamines
qDIL	Quaternary Diltiazem
I	Current
I-V	Current-voltage
$V_{0.5act}$	Voltage of half-maximal current activation
$V_{0.5inact}$	Voltage of half-maximal current inactivation
qDev	Quaternary devapamil
IC_{50}	Concentration for 50% inhibition
act	Time constant of current activation
inact	Time constant of current inactivation
r300	Inactivation during a 300-ms pulse

(Dedicated) To my father, the late Shabbir Hussain

Abstract

Calcium fluxes through $Ca_V1.2$ (L-type) channels determine cellular excitability and initiate contractions of muscle cells, release of hormones and neurotransmitters from secretory and nerve cells, gene expression, and many other cellular processes. A drug that blocks calcium influx through $Ca_V1.2$ is the benzothiazepinone (BTZ) diltiazem. Although diltiazem has been in clinical use for a long time, its molecular mechanisms and its access pathway to its binding site in $Ca_V1.2$ are not fully understood. To identify the access route of diltiazem to its putative binding site, the quaternary diltiazem analog qDil was synthesised and applied to either the extra- or intracellular site of the membrane. Intracellularly applied qDil induced a concentration- and use-dependent block suggesting an intracellular access path. During my studies a novel high affinity qDil binding site was identified by molecular modelling and mutational analysis. Substitution of threonine to alanine in position 1143 (T1143A) of the α1-subunit of $Ca_V1.2$ diminished the qDil block at low (0.2Hz) as well as high frequency (1Hz) depolarization pulses. Mutation T1143A also reduced channel block by the clinically used tertiary diltiazem and a quaternary PAA (qDevapamil). T1143A affected neither activation nor inactivation of $Ca_V1.2$, supporting the view that this residue forms part of the diltiazem binding pocket on $Ca_V1.2$.

Zusammenfassung

Der Einstrom von Calcium durch spannungsabhängige $Ca_v1.2$ Kanäle reguliert Erregung und Kontraktilität der Muskulatur, die Freisetzung von Hormonen und Neurotransmittern aus sekretorischen Zellen oder Nervenzellen und eine Vielzahl anderer zellulärer Prozesse. Dieser Calciumeinstrom kann durch Calciumkanalantagonisten dreier verschiedener Klassen, Phenylalkylamine (PAA), 1,4 Dihydropyridine (DHPs), und Benzothiazepine (BTZs) inhibiert werden. Diltiazem (Dil), ein Vertreter der Benzothiazepine, wird bereits lange Zeit therapeutisch verwendet. Bislang konnten jedoch die molekularen Wirkungsmechanismen und der Zugangsweg („access path“) von Diltiazem zu seiner hochaffinen Bindungsstelle in Cav1.2 nicht geklärt werden. Um den extra- bzw. intrazellulären Zugang von Dil zu seiner Bindungsstelle zu untersuchen, wurde das quaternäre Diltiazem-Analogon *qDil* synthetisiert und entweder extrazellulär oder intrazellulär appliziert. Die intrazelluläre Applikation erzeugte einen konzentrationsabhängigen ‚Use-dependent Block‘, was einen intrazellulären Zugang zur Bindungsstelle nahelegt. Darüber hinaus konnte durch meine Studien mittels Mutationsanalyse und molekularem Modeling eine neue, hoch affine, Bindungsdeterminante von Dil identifiziert werden. Die Substitution von Threonin durch Alanin an der Position 1143 (T1143A) im $Ca_v1.2$ verringert den Block von *qDil* sowohl bei nieder- (0,2 Hz) als auch hochfrequenten (1 Hz) Depolarisationspulsen. Außerdem reduziert T1143A den Block von dem klinisch verwendetem tertiären Diltiazem und quarternären Phenylakylaminen (qDevapamil). T1143 hatte weder Einfluss auf die Aktivierung noch die Inaktivierung der $Ca_v1.2$ Kanäle. Die reduzierte Wirkung von Dil an der T1143A Mutante ist somit nicht über allosterische Mechanismen (Konformationsänderungen des Moleküls) zu erklären. Diese Befunde stützen die Hypothese, dass T1143 eine wichtige Bindungsdeterminante von Dil auf Cav1.2 darstellt.

1 CHAPTER I

1.1 Discovery and cellular role of calcium channels

Voltage-dependent calcium channels (VDCC) are membrane proteins that are key transducers of electrical signaling. They convert the depolarization of the cell membrane into an influx of calcium ions into the cell. This incoming calcium initiates a large variety of cellular events such as action potentials, excitation-contraction coupling, neurotransmission, secretion, gene expression and others (Catterall 2000). These channels are ubiquitously distributed throughout cellular life. The influx of calcium through them is very crucial for the maintenance of cellular homeostasis and other regulatory events. Calcium channels are expressed in excitable cells (nerve, muscle) but are also found in many cells that are not traditionally considered excitable, e.g cells of the immune system (Cahalan et al. 2001). Paul Fatt and Bernard Katz first identified calcium channels in crustacean muscle, when they left the Na^+ out of their bathing medium and found that the muscle still generated action potentials (Fatt and Katz 1953). Harald Reuters was the first to record the calcium current in Purkinje fibers under voltage clamp (Reuter 1967).

1.2 Classification of calcium channels

Initially, two main types were distinguished on the basis of their voltage dependence and electrophysiological properties in low-voltage activated (LVA) and high-voltage activated (HVA) calcium channels. First evidence of these two distinct types of voltage-gated calcium channels came in 1975 from experiments of Hagiwara, Ozawa and Sand with the two-microelectrode voltage-clamped method on starfish eggs (Hagiwara et al., 1975). They

demonstrated that calcium channels are activated by small depolarizations of the membrane (LVA) and large depolarizations of the membrane (HVA) (Hagiwara et al, 1975). Until now 10 genes have been identified encoding α1-subunits of voltage-gated calcium channels. Alignment of their deduced amino acid sequences suggests that gene duplication and divergence of an ancestral calcium channel gene gave rise to LVA and HVA subfamilies and Ca_v1 and Ca_v2 subfamilies arose from further duplication of the HVA gene (Perez-Reyes 2003).

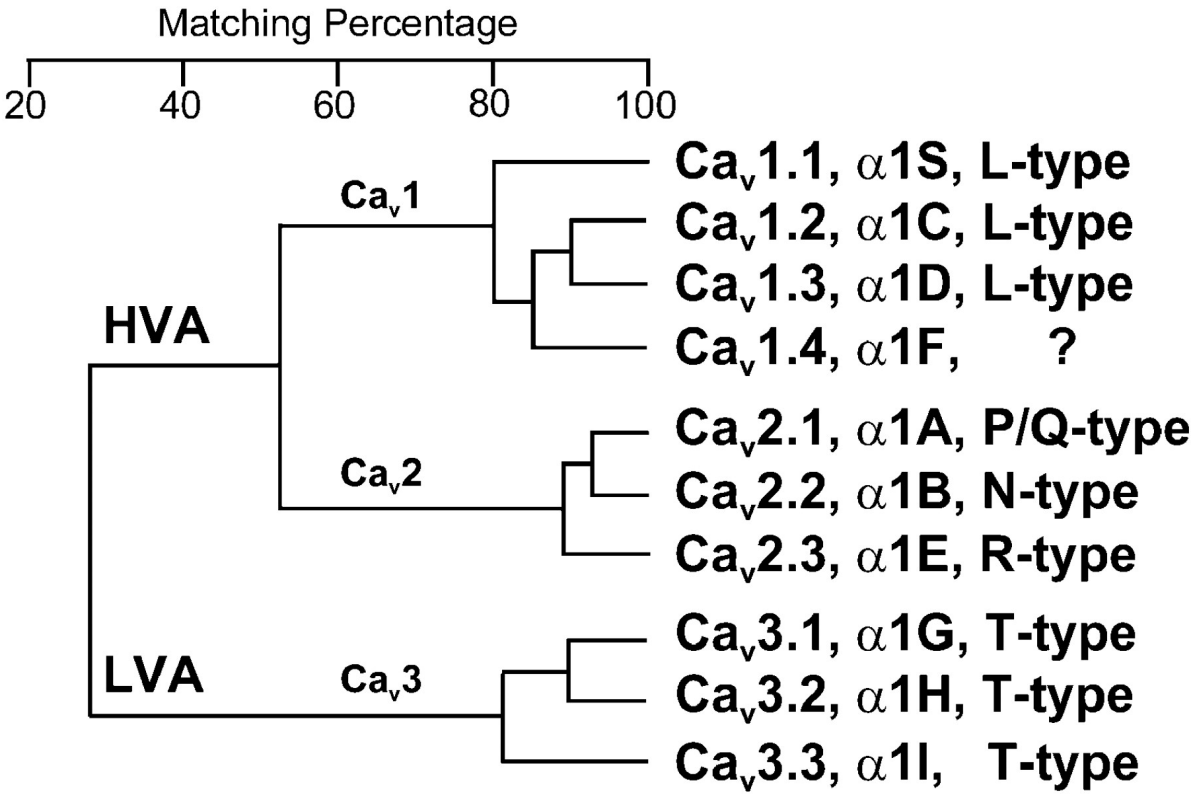

Figure 1. Evolutionary tree of voltage-gated Ca^{2+} channels

*Figure adapted from Perez-Reyes (2003)

In 1982, Tsien et al. subdivided calcium channels into three distinct classes on the basis of their slope conductances and activation and inactivation properties. The different classes were named T-type (LVA), N-type and L-type (both HVA) channels. The L-type channels display a large unitary conductance for Ba^{2+}, supporting long-lasting channel openings and are found in myocardial cells (Reuter et al. 1982). The T-type channels conduct tiny (small amplitude)

unitary currents giving rise to a transient average current with a characteristically slow deactivation following sudden depolarization (Armstrong and Matteson 1985) and also were shown in heart cells (Nilius et al. 1985). Lastly, the N-type channels were found in neurons, they had an intermediate conductance to Ba^{2+} (Williams et al. 1992).

Table 1: Detailed characteristics of calcium channels

Channel Protein	**Calcium current**	**Gene Name and Human chromosome**	**Localization**	**Specific antagonist**	**Cellular functions**
Ca_v 1.1	L	CACNA 1S 1q31-32	Skeletal muscle; transverse tubules	Dihydropyridines Phenylalkylamines Benzothiazepines	Excitation contraction coupling
Ca_v1.2	L	CACNA 1C 12p13.3	heart smooth muscle brain heart pituitary adrenal	Dihydropyridines Phenylalkylamines Benzothiazepines	Excitation-contraction coupling, hormone release; regulation of transcription; synaptic integration
Ca_v 1.3	L	CACNA 1D 3p14.3	brain, pancreas, kidney, ovary, cochlea	Dihydropyridines Phenylalkylamines Benzothiazepines	Hormone release; regulation of transcription; synaptic regulation; cardiac pacemaking; hearing neurotransmitter release from sensory cells
Ca_V1.4	L	CACNA 1F Xp11.23	Retinal rod and bipolar cells; spinal cord; adrenal gland; mast cells	Dihydropyridines Phenylalkylamines Benzothiazepines	Neurotransmitter release from photoreceptors
Ca_V2.1	P/Q	CACNA 1A 19p13	Nerve terminals and dendrites; neuroendo-crine cells	ω-Agatoxin IVA	Neurotransmitter release; dendritic Ca^{2+} transients hormone release

$Ca_V2.2$	N	CACNA 1B 9q34	Nerve terminals and dendrites; neuroendo-crine cells	ω-Conotoxin-GVIA	Neurotransmitter release; dendritic Ca^{2+} transients hormone release
$Ca_V2.3$	R	CACNA 1E 1q25-31	Neuronal cell bodies and dendrites	SNX-482	Repetitive firing; dendritic calcium transients
Ca_V 3.1	T	CACNA 1G 17q22	Neuronal cell bodies and dendrites; cardiac and smooth muscle myocytes	None	Pacemaking repetitive firing

* Table from Ertel et al. (2000), with changes

1.2.1 Cardiac L-VGCC structure

The L-VGCCs are transmembrane protein complexes comprising the pore forming α1, and auxiliary α2δ, β, and, in some tissues, γ subunits Fig 2. Upon membrane depolarization they allow calcium influx into the cell (Catterall 2000). In excitable tissues, Ca^{2+} channels invariantly contain α1, α2δ, β, subunits. The accessory subunits α2δ, β, are sparingly bound to the α1 subunit and modulate the biophysical properties and promote trafficking of the α1 subunit to the membrane (Brice et al. 1997, Singer et al. 1991, Meir and Dolphin 2002).

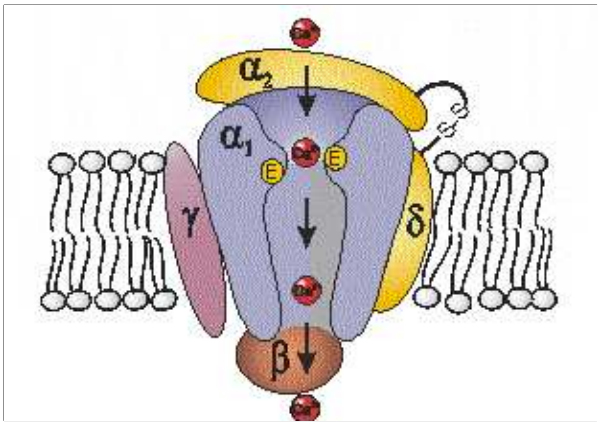

Figure 2. Schematic structure of VGCC

The principal α1-subunit is a transmembrane protein containing a conducting pore, lined with highly conserved glutamate residues. Passage of calcium ions upon opening of the α1-subunit is further regulated by auxiliary subunits: the intracellular β-subunit, the transmembrane γ-subunit and a complex of the extracellular α2-subunit and the transmembrane δ-subunit, connected by a disulfide bridge.

*Image adapted from: www.ipt.med.tu-muenchen.de

Cardiac contraction is initiated by the influx of calcium through L-type calcium channels (LTCC) of transverse tubules (T-tubules) in the cell membrane. The small amount of Ca^{2+} influx through LTCC triggers a large-scale Ca^{2+} release from the sarcoplasmic reticulum (SR) through ryanodine receptors (RyR2) (Bers 2002). Calcium then associates with troponin C in

the sarcomere and stimulates contraction (systole). The increase in cytoplasmic Ca^{2+} concentration will induce muscle contraction. To enable relaxation, intracellular Ca^{2+} is pumped back into the SR via SR Ca^{2+}-ATPase (SERCA2a), which is regulated by phospholamban (PLB), or extruded from the cell via the Na^{+}/Ca^{2+}-exchanger (Bers 2002) (Fig 3).

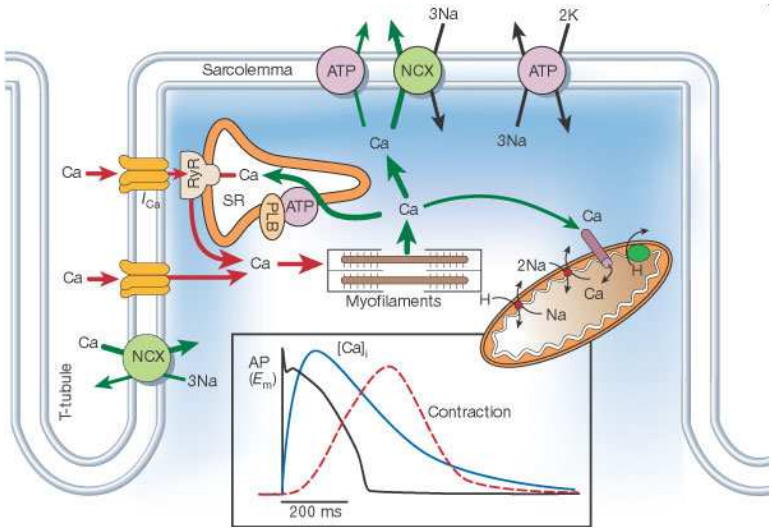

Figure 3. Ca^{2+} transport in ventricular myocytes.

The inset shows the time course of action potential, Ca^{2+} transient and contraction measured in a rabbit ventricular myocyte at 37 °C. NCX, Na^{+}/Ca^{2+} exchange; ATP, ATPase; PLB, phospholamban; SR, sarcoplasmic reticulum.

*Figure adapted from Bers (2002)

1.2.2 L-type ($Ca_V1.2$) channels

Detailed properties of L-type calcium channels are given in Table 2.

Properties of L-type (CaV1.2) channels

Channel name	$Ca_V1.2$
Description	Voltage-gated calcium channel with α_1-subunit. Other names: α_{1C}, muscle dihydropyridine receptor.
Molecular information	Human: 2169aa, L29529 (cardiac; PMID: 8392192), 2138aa, Z34815 (fibroblast; PMID: 1316612); 2138aa, AF465484 (jejunum; PMID: 12176756); chr. 12p13.3, *CACNA1C*, LocusID: 775 Rat: 2169aa, M59786 (aortic smooth muscle; PMID: 2170396); 2140/2143aa, M67516/M67515 (brain; PMID: 1648941); chr. 4q42, Cacna1c, LocusID: 24239 Mouse: 2139aa, L01776 (brain; PMID: 1385406); chr. 6, Cacna1c, LocusID: 12288 (see 'Comments'
Associated subunits	$\alpha_2\delta$, β, γ
Functional assays	Patch-clamp (whole-cell, single-channel), calcium imaging, cardiac or smooth muscle contraction hormone secretion
Current	$I_{Ca,L}$
Conductance	Ba^{2+} (25pS) > Sr^{2+} = Ca^{2+} (9pS)
Ion selectivity	Ca^{2+} > Sr^{2+} > Ba^{2+} >> Mg^{2+} from permeability ratios
Activation	V_a = –17 mV (in 2 mM Ca^{2+}; HEK cells); –4 mV (in 15 mM Ba^{2+}; HEK n 5 mM Ba^{2+}; HEK cells and *Xenopus* oocytes); τ_a = 1 ms at +10 mV
Inactivation	V_h = –50 to –60 mV (in 2 mM Ca^{2+}; HEK cells), –18 to –42 mV (in 5-15 mM Ba^{2+}; HEK cells); τ_{fast} = 150 ms, τ_{slow} = 1100 ms; 61% inactivated after 250 ms in HEK cells (at V_{max} in 15 mM Ba^{2+}); 70% inactivation after 1 s (at V_{max} in 2 mM Ca^{2+}); inactivation is accelerated with Ca^{2+} as charge carrier (calcium-dependent inactivation: 86%

	inactivated after 250 ms)
Activators	BayK8644, dihydropyridine agonists, FPL64176
Gating modifiers	Dihydropyridine antagonists (e.g., isradipine, IC_{50} = 7 nM at –60 mV; nimodipine, IC_{50} = 139 nM at –80 mV)
Blockers	Nonselective: Cd^{2+} ; selective for $Ca_V1.x$: devapamil (IC_{50} = 50 nM in 10 mM Ba^{2+} at –60 mV) and other phenylalkylamines; diltiazem (IC_{50} = 33 μM in 10 mM Ba^{2+} at –60 mV and 0.05Hz)
Radioligands	(+)-[^{3}H]isradipine (K_d < 0.1 nM) and other dihydropyridines; (–)-[^{3}H]devapamil (K_d = 2.5 nM), (+)-*cis*-[^{3}H]diltiazem (K_d = 50 nM)
Channel distribution	Cardiac muscle, smooth muscle (including blood vessels, intestine, lung, uterus); endocrine cells (including pancreatic β-cells, pituitary); neurones; subcellular localization: concentrated on granule-containing side of pancreatic β-cells; neurons (preferentially somatodendritic)
Physiological functions	Excitation-contraction coupling in cardiac or smooth muscle, action potential propagation in sinoatrial and atrioventricular node, synaptic plasticity, hormone (e.g., insulin) secretion
Mutations and pathophysiology	Required for normal embryonic development (mouse, zebrafish); de novo G406R mutation in alternative exon 8A in 1 allele causes Timothy syndrome[20]
Pharmacological significance	Mediates cardiovascular effects of clinically used Ca^{2+} antagonists; high concentrations of dihydropyridines exert antidepressant effects through $Ca_v1.2$ inhibition
Comments	Tissue-specific splice variants exist; in addition to cardiac channels, smooth muscle and brain channels have been cloned; the gene for $Ca_v1.2$ was first isolated and characterized in rabbit heart (2171aa, P15381, X15539)

From international Union of Pharmacology. XLVIII. Nomenclature and Structure-Function Relationships of Voltage-Gated Calcium Channels

William A. Catterall, Edward Perez-Reyes, Terrance P. Snutch, and Joerg Striessnig, Pharmacol. Rev. 2005 57: 411-425

aa, amino acids; chr., chromosome; HEK, human embryonic kidney.

* Table from Catterall et al (2005)

1.1 Purification of L-type channels

Purification of Ca^{2+} channels skeletal muscle began with isolation of the Ca^{2+} channel protein from transverse tubule membranes, in an approach to use high-affinity binding to dihydropyridine Ca^{2+} channel antagonists to identify the channel protein (Borsotto et al. 1985; Curtis and Catterall 1984). To avoid native subunit associations, Ca^{2+} channels were solubilized in a mild detergent and subsequently purified by a combination of ion-exchange chromatography, affinity chromatography on wheat-germ agglutinin Sepharose, and sedimentation through sucrose gradients (Curtis and Catterall 1984). A heterogeous α-subunit band (Borsotto et al. 1985; Curtis and Catterall 1984), 50-kDa associated β-subunits and 33-kDa γ-subunits were identified as components of the Ca^{2+} channel in the initial purification studies. Later studies demonstrated that the heterogenous α-subunit band contained not only the main α1-subunits with an obvious molecular mass of 175 kDa but also a disulfide-linked dimer of α2-δ subunits with apparent molecular masses of 143 kDa and 27 kDa, respectively, as illustrated in the SDS-PAGE in Fig 4A (Hosey et al. 1987; Leung et al. 1987; Sieber et al. 1987; Takahashi et al. 1987b; Vaghy et al. 1987).

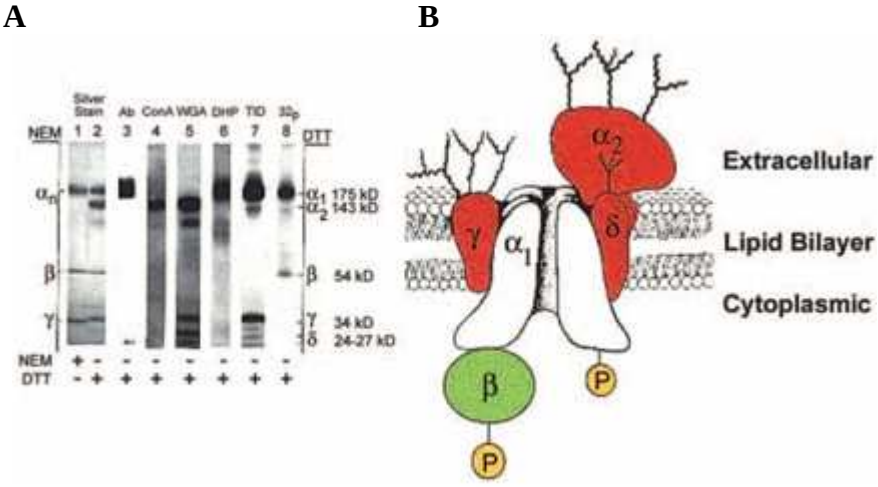

Figure 4. Biochemical properties of skeletal muscle Ca^{2+} channels

A. Summary of the biochemical properties of purified skeletal muscle Ca^{2+} channels. Lanes 1 and 2, silver stain of polypeptides; lane 3, staining with an antibody against the α1-subunit; lane 4, staining with concanavalin A, a lectin binding high mannose N-linked carbohydrate chains; lane 5, staining with wheat germ agglutinin, a lectin staining N-linked complex carbohydrate chains; lane 6, photoaffinity labeling with azidopine, a photoreactive dihydropyridine; lane 7, photoaffinity labeling with TID, a hydrophobic probe of the transmembrane regions of proteins; lane 8, phosphorylation by cAMP-dependent protein kinase (Takahashi et al., 1987). B. The subunit structure of Ca^{2+} channels purified from skeletal muscle is illustrated. The model is updated from the original description of the subunit structure of skeletal muscle Ca^{2+} channels Takahashi et al., (1987).

*Figure adpted from Catterall, Landes Bioscience; (2000)

1.2 Calcium channel subunits

1.2.1 Alpha1C

The α1-subunit of skeletal muscle Ca^{2+} channels was cloned by library screening based on amino acid sequence (Tanabe et al. 1987). The calcium channel α1-subunit 170-240 kDa consists of 4 homologous motifs (I-IV), each composed of 6 membrane-spanning α-helices

(termed S1 to S6) linked by variable cytoplasmic loops (linkers) between the S5 and S6 segments Fig. 5 (Bodi et al. 2005). To date, 10 α1 subunit coding genes have been identified and separated into four classes: $Ca_V1.1$ (α1S), 1.2 (α1C), 1.3 (α1D), and 1.4 (α1F) (see also Table 1). Only the α1C (dihydropyridine-sensitive [DHP-sensitive]) subunit is expressed in high levels in cardiac muscle. $Ca_V2.1$ (α1A), 2.2 (α1B), and 2.3 (α1E) form P/Q-, N-, and more likely R-type channels, respectively, and are all found specifically in brain (Bodi et al. 2005). They are principally responsible for synaptic transmission initiation at fast synapses in the nervous system (Yokoyama et al. 2005).

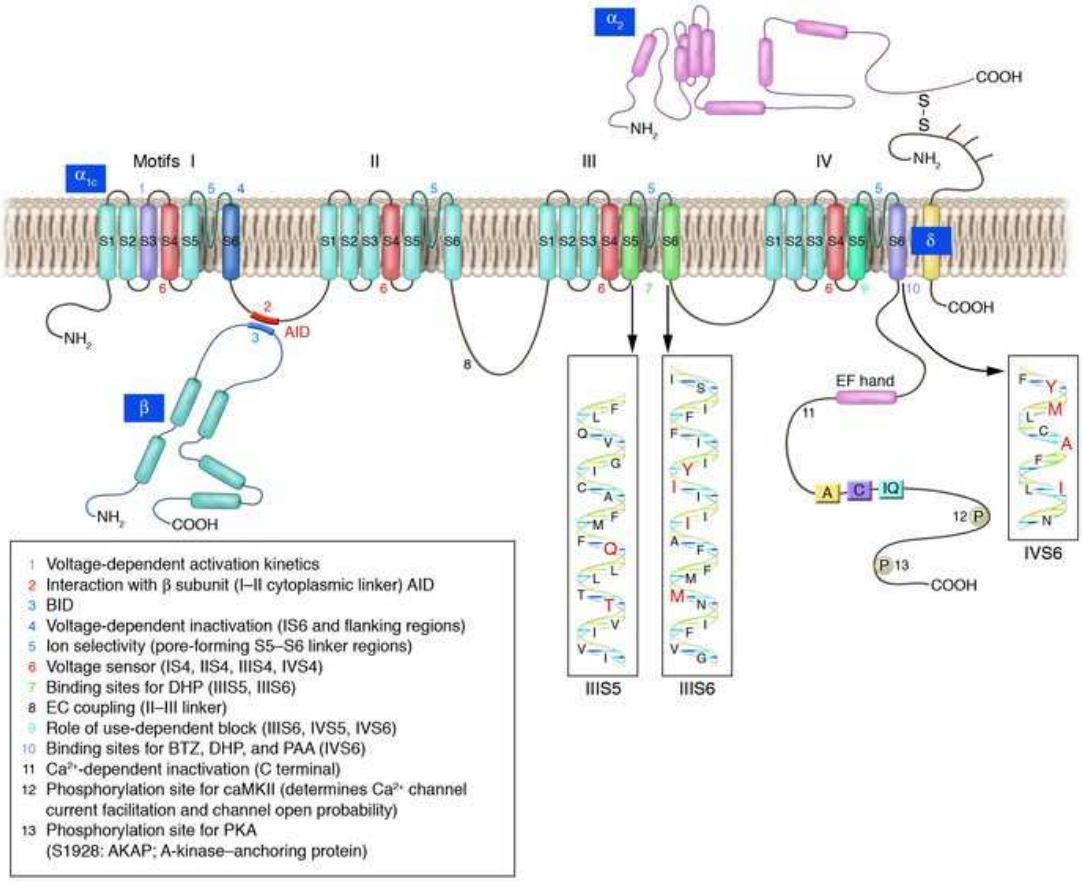

Figure 5. Structural organization of L-VGCCs

The membrane topological architecture of the core subunits, the auxiliary subunits with structural domains, and their interactions which are common to all VGCC types, are shown. The main structure of the pore forming α1 subunit is composed of four homologous repeating domains (I–IV), each of which consists of six putative transmembrane motifs (S1–S6). The cytoplasmic loops are usually named according to the domains they link.

*Figure adapted from Bodi et al (2005)

The α1 subunit form the ion-conducting pore, contains gating machinery, voltage sensor, and the drugs binding sites (Carafoli et al. 2001; Catterall 2000; Takahashi and Catterall 1987). The pore has high affinity with Ca^{2+} ions due to conserved glutamate (EEEE) which are arranged in asymmetric manner (Klockner et al. 1996; Koch et al. 2000; Mikala et al. 1993). The fourth transmbrane segment of each motif is positively charged highly conserved, and is likely to form an α-helix containing every third or fourth basic (Arg or Lys) residue (Bezanilla 2002).

1.2.2 Sites of protein phosphorylation

The α1-subunits of skeletal muscle Ca^{2+} channels are substrates for phosphorylation by cAMP-dependent protein kinase and a number of other protein kinases (Curtis and Catterall 1985; Jahn et al. 1988; Nastainczyk et al. 1987; O'Callahan et al. 1988). It has been shown that cAMP-dependent protein kinase phosphorylates skeletal muscle L-type Ca^{2+} channels and enhances their activation (Arreola et al. 1987; Schmid et al. 1985). Repetitive depolarization of cultured skeletal muscle cells causes a dramatic cAMP-dependent potentiation of Ca^{2+} currents (Fleig and Penner 1996; Sculptoreanu et al. 1993). Increases in both the number of functional Ca^{2+} channels and in the activity of single Ca^{2+} channels were detected after phosphorylation by cAMP-dependent protein kinase in single-channel recording experiments in planar bilayer membranes (Flockerzi et al. 1986; Hymel et al. 1988). Thus, the α1-subunit of the purified Ca^{2+} channel contains the sites at which cAMP-dependent protein phosphorylation modulates channel function in vitro (Catterall 2000).

Regarding phosphorylation sites, earlier it was shown that Ser 687, located in the intracellular loop between domains II and III, is the most rapidly phosphorylated site in the truncated form of the α1-subunit in purified Ca^{2+} channel preparations (Rohrkasten et al. 1988; Rotman et al. 1992). Whereas later, it was clearly revealed in time-course experiments that a Ser1854 near

the C-terminal portion of full-length α1212 is the most intensely and rapidly phosphorylated (Rotman et al. 1995).

1.2.3 Beta subunits

The β-subunits are hydrophilic proteins that are not glycosylated and therefore are likely to be located on the intracellular side of the membrane Fig 5 (Takahashi et al. 1987). The first $Ca_V\beta$ subunit to be identified, now called $Ca_V\beta 1$*a,* was observed as a 54 kDa subunit in the purified skeletal muscle DHP receptor calcium channel complex (Takahashi et al. 1987b) and its gene was cloned following partial sequencing of the protein (Ruth et al. 1989). The existence of four different β genes (β_1-β_4) and extensive differential splicing, especially of β_1 and β_2 transcripts, give rise to multiple isoforms (Foell et al. 2004). The β subunit is firmly bound to a highly conserved motif in the cytoplasmic linker between repeats I and II (AID) of all cloned high voltage–gated α1 subunit isoforms, via an 18 amino acid motif called the α-interaction domain (AID) Fig 4 (Pragnell et al. 1994), and also to a secondary site (Opatowsky et al. 2003). On the β-subunit, a 41-amino acid sequence beta interaction domain (BID) was identified as the minimal sequence required to drive α_1 subunit expression (de Waard and Rooijers 1994).

1.2.3.1 Roles of beta (β2) subunits in calcium channel assembly and trafficking

It has been shown that the beta subunit has marked effects on the properties of HVA α_1-subunits including current amplitude, modification of channel kinetics, and targeting of complex to the plasma membrane (Brice et al 1997, Singer et al 1991). The antisense-induced depletion of $Ca_V\beta$ subunits from Dorsal root ganglia (DRGs) results in a reduction of amplitude of endogenous calcium currents, and slowed kinetics of activation (Berrow et al 1995, Campbell et al 1995).

It has been demonstrated that all $Ca_V\beta$-subunits enhance the functional expression of HVA α1-subunits (Birnbaumer et al. 1998). This could in theory attributed to an increase in the open probability, single-channel conductance, number of functional channels inserted into the plasma membrane, or a combination of several processes (Dolphin 2003).

Initially there was some controversy concerning the effect of $Ca_V\beta$ subunits on the number of channels in the plasma membrane. For instance, initial studies in *Xenopus* oocytes showed that for $Ca_V1.2$ and $Ca_V2.3$, the $Ca_V\beta$-subunits had no effect on the voltage-dependence of charge movement (visualized as gating current), and did not increase the total amount of charge transferred, which is a measure (indication) of the number of voltage sensors moving in the membrane, and therefore of channels inserted into the membrane (Olcese et al. 1996). However, it was found that β-subunits hyperpolarized the voltage dependence of the ionic current (Olcese et al. 1996). Thus, the β subunits produced an increase in the ratio of charge movement to ionic current, and were said to improve the coupling between voltage sensor movement and channel opening (Neely et al. 1993; Olcese et al. 1996). In contrast, other groups have found that co-expression of a β-subunit did increase the charge movement associated with $Ca_V1.2$ gating (Colecraft et al. 2002; Josephson and Varadi 1996). Furthermore, many groups have found that $Ca_V\beta$-subunits have a chaperone like effect, promoting functional expression of the $Ca_V2.1$, 2.2, and 2.3 subunits at the plasma membrane of mammalian cells, and increasing localization of the channels at the plasma membrane (Bichet et al. 2000; Brice et al. 1997; Raghib et al. 2001; Yamaguchi et al. 1998). Recently it was shown that an increase of (rat brain) $Ca_V1.2$ channel density was positively influenced by PI3K and β2a (Viard et al. 2004). It was shown that β1-KO mice suffer from impaired EC coupling and early lethality (Gregg et al. 1996), clearly indicate that β1 subunit is crucial in EC coupling. The exact mechanism of EC coupling is still not fully understood, but it is possible that the deficiency in the assembly process of the α1/β1 complex results in the degradation of the α1 subunit (Gregg et al. 1996). The role of the β2 subunit in EC coupling

is unclear (S. L. Ball et al., 2002) and β3-null mice have no detectable abnormalities in the heart (Murakami et al. 2000).

Different splice variants of the β subunits namely β2a and β2b, have been shown to regulate Cav1.2 function (Chien et al. 1996; Qin et al. 1998) .

1.2.3.2 Effect of beta subunit on voltage dependence of calcium channels

It is well established that all β-subunits affect the voltage dependence of activation of all HVA calcium channels (Birnbaumer et al. 1998; Canti et al. 2000; Jones et al. 1998).

For steady-state inactivation differences are apparent, both between different α1-subunits and different β-subunits. There is little difference between different β-subunits and splice variants in their ability to shift the steady-state inactivation for $Ca_V1.2$ (Jones et al. 1998; Takahashi et al. 2003). In contrast, all except palmitoylated β2a hyperpolarize the voltage dependence of steady-state inactivation for $Ca_V2.3$ and $Ca_V2.3$ (Birnbaumer et al. 1998; Canti et al. 2000; Jones et al. 1998).

1.2.3.3 Effect of beta subunit on calcium channel gating

It was reported that β-subunits influence all kinetic processes and have a marked effect on open probability, largely by reducing the mean closed time (Colecraft et al. 2002). In case of $Ca_V2.3$ the kinetics of current activation are little affected by the expression of different β-subunits (Jones et al. 1998; Meir and Dolphin 2002). It was also observed by other groups that for $Ca_V2.2$ single channels, the distribution of latencies to first opening of $Ca_V2.2$ channels and the mean open and closed times were similar for both β1b and β2a-subunits (Meir and Dolphin 2002). However, the inclusion of the β2a-subunit led to channels with an additional phase of slow activation, which may represent slow exit from an inactivated state (Meir and Dolphin 2002).

As VDCC α1-subunits contain inherent determinants of voltage-dependent inactivation (Cens et al. 1999; Herlitze et al. 1997; Spaetgens and Zamponi 1999; Zhang et al. 1994), association with different β subunit isoforms dictates their overall inactivation rate (Meir and Dolphin 2002; Olcese et al. 1994). With HVA at the whole cell level, coexpression of β1b, β2a, β2e, or β4 subunits generally decreased the inactivation rate, whereas β3 enhanced inactivation, compared to the α1-subunit expressed alone (Dolphin 2003).

1.2.3.4 Effect of beta subunits on calcium channel pharmacology

Many drugs, such as verapamil and mibefradil, bind preferentially to inactivated calcium channels, and therefore their ability to inhibit the channels will be indirectly affected by the β-subunit complement because of their differential effects on inactivation (Berjukow et al. 2000; Lacinova et al. 1995; Zamponi et al. 1996).

1.2.4 α2-δ-subunits

During purification of skeletal muscle calcium channels, a disulfide-linked dimer of α2-δ subunits, with apparent molecular masses of 143 kDa and 27 kDa, respectively, was seen (Hosey et al. 1987; Leung et al. 1987; Sieber et al. 1987; Takahashi et al. 1987a; Vaghy et al. 1987). Protein sequencing has shown that α2 and δ are the product of a single gene, termed the α2δ gene, and are separated by proteolytic cleavage (De Jongh et al. 1990; Ellis et al. 1988; Jay et al. 1991). Until now, four genes encoding α2-δ-subunits have been identified and cloned α2/δ1, 2, 3, 4 (De Jongh et al. 1990; Qin et al. 2002). α2δ-1 was initially cloned from skeletal muscle and showed a fairly ubiquitous distribution (Barclay et al. 2001; Ellis et al. 1988; Gao et al. 2000; Qin et al. 2002). It possesses a high-affinity binding site for gabapentin (GABA-antagonists), which are widely used to treat epilepsy, sleep disorders, pain, and many other neurological conditions (Luo et al. 2002; Marais et al. 2001; Sutton et al. 2002). The α2δ-2 cloned from brain has also some affinity for gabapentin (Bodi et al.

2005). α2/δ2 deficient mice exhibit neurological dysfunction, such as enhanced seizure susceptibility and cardiac abnormalities, namely a liability to develop bradycardia (Ivanov et al. 2004). α2δ-3 subunits were also cloned from brain (Barclay et al., 2001: Klugbauer et al., 1999; Qin et al., 2002). The human α2/δ4 subunit (is localized in colon, fetal liver, pituitary, and adrenal gland) is associated with the $Ca_V1.2$ α1C and β3 subunits (Qin et al., 2002). Several reports have shown that α2δ-subunits increase the expression of many HVA α1- and β-subunit combinations, and all α2δ-subunits seem to have similar effects on current amplitude (Canti et al 2003). For example, the peak $Ca_V1.2$ current amplitude is increased threefold by coexpression of α2δ (Felix et al., 1999). Also, α2δ-1 increases the amount of $Ca_V1.2$ subunit protein associated with the plasma membrane in *Xenopus* oocytes used for heterologous expression (Shistik et al. 1995). α2δ-2 increases $Ca_V2.2$, $Ca_V2.1$ and $Ca_V1.2$ currents by about threefold in both mammalian cells and *Xenopus* oocytes (Canti and Dolphin 2003; Canti et al. 2005; Davies et al. 2006; Gao et al. 2000). Knock out of full-length α2δ-2 produced an epileptic and ataxic phenotype (Barclay et al. 2001; Meier 1968), another link between α2δ-subunits and disease relates to their involvement in neuropathic pain. It was shown that both α2δ-1 and α2δ-2 are present in rat dorsal root ganglion neurons (DRGs) (Cole et al. 2005), and there is an upregulation of α2δ-1 protein and mRNA both in DRGs and in spinal cord on the same side as an experimental nerve crush injury (Luo et al. 2001; Newton et al. 2001; Wang et al. 2002). This upregulation correlates with the onset of allodynia, in which the sensation of non-noxious touch causes pain-related behaviours, and subsequent downregulation correlates with the gradual loss of allodynia in this model (Devies et.al. 2007). In addition, intrathecal administration of antisense oligonucleotides directed against α2δ-1 mRNA reduces both the experimental upregulation of protein and pain-related behaviours (Li et al. 2004). It has recently been shown that mice overexpressing α2δ-1 show allodynia in the absence of nerve injury (Li et al. 2006).

1.2.5 The γsubunits

The γ-subunit of skeletal muscle Ca^{2+} channels is a hydrophobic glycoprotein with an apparent molecular mass of 30kDa without deglycosylation and 20kDa following deglycosylation (Sharp and Campbell 1989; Takahashi et al. 1987b). To date, 8 genes encoding gamma subunits γ_1-γ_8 have been identified (Kang and Campbell 2003).

1.3 Calcium channel antagonists targeting L-type calcium channels

Calcium channel antagonists (CA) are a chemically, pharmacologically and therapeutically heterogeneous group of drugs prominent both as cardiovascular therapeutic agents and as molecular tools (Triggle 2007). The calcium channel blockers are divided into three main classes: phenylalkylamines (PAA; e.g. verapamil), dihydropyridines (DHP; e.g. nifedipine) and benzothiazepines (BTZ; e.g. diltiazem). Each of these three types of drug has separate, but overlapping or allosterically linked, Ca^{2+} channel–binding sites on the IIIS6 and IVS6 binding motifs (Fig. 5).

The cardiovascular activities of these drugs as antihypertensive, antianginal and selective antiarrhythmic agents are due to their action on one particular calcium mobilization process: calcium entry through an L-type voltage-gated calcium channel (Triggle 2007). Many studies have demonstrated that in accord with their chemical heterogeneity these agents interact at discrete receptor sites associated with a major subunit of the channel Fig. 6 (Triggle 2007).

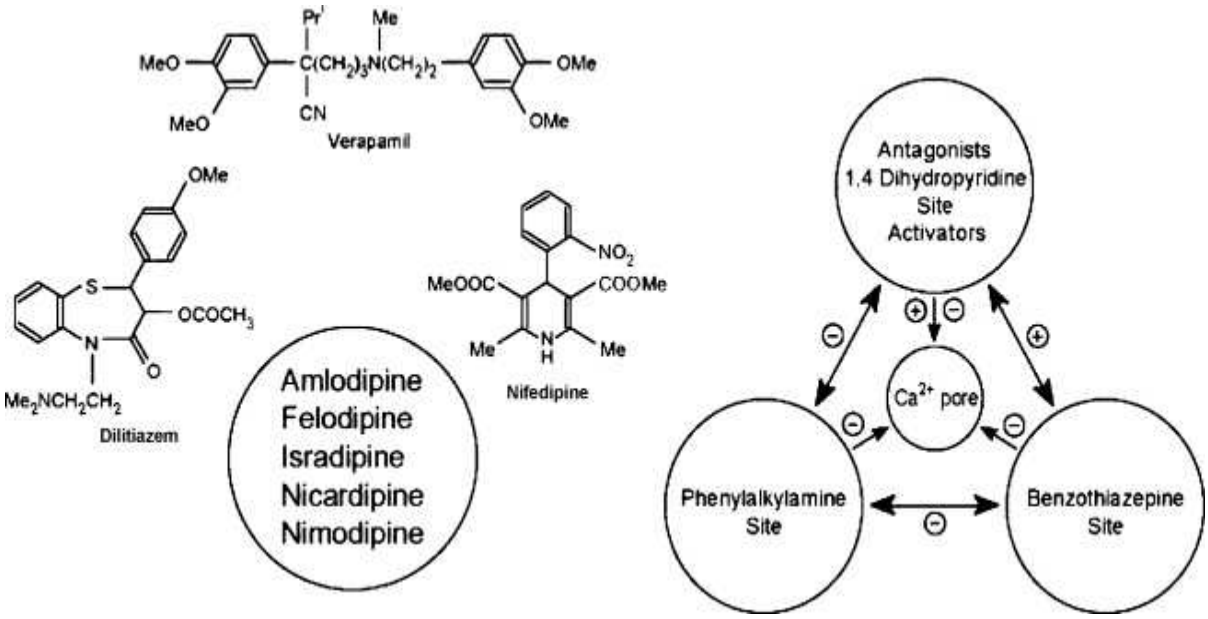

Figure 6. Ca^{2+} channel antagonist interactions at the L-type voltage-gated calcium channel

In this schematic representation the three major structural classes of drug are shown interacting at separate but allosterically linked receptor sites. The drugs depicted in the circle are second-generation 1,4-dihydropyridines and include the widely prescribed amlodipine (Norvasc™). *Figure from Triggle (2007)

1.4 Use-dependent block

The normal operation of voltage-gated calcium channels involves conformational changes large enough to switch between states with completely open or completely closed water-filled pores. These switches between the *gating states (resting, open, inactivated)* typically occurs on a millisecond time scale in response to changes in membrane voltage and are often accompanied by dramatic changes in drug binding affinity.

A use-dependent pattern is described where peak I_{Ca} is progressively reduced by a train of depolarizing test pulses since inhibition increases as channels are “used” by cycling through various gating states during the action potentials. The more frequently the Ca^{2+} channel opens, the better is the penetration of the drug to the binding site (see Hering et al. 1997 for PAA action). Since then, single amino acids have been identified as inactivation determinants in motifs IIIS6, IVS6, and IVS5, with some of them also serving as high-affinity

determinants for the DHP receptor site (Benitah et al. 2002; Hering et al. 1998; Motoike et al. 1999), BTZ binding site (Hockerman et al. 2000) and PAA binding site (Hering et al., 1997; Hockerman et al., 1995; Hockerman et al., 1997b).

1.5 References

Armstrong, C. M., and Matteson, D. R. (1985). Two distinct populations of calcium channels in a clonal line of pituitary cells. Science *227*, 65-67.

Arreola, J., Calvo, J., Garcia, M. C., and Sanchez, J. A. (1987). Modulation of calcium channels of twitch skeletal muscle fibres of the frog by adrenaline and cyclic adenosine monophosphate. J Physiol *393*, 307-330.

Ball, S. L., Powers, P. A., Shin, H. S., Morgans, C. W., Peachey, N. S., and Gregg, R. G. (2002). Role of the beta(2) subunit of voltage-dependent calcium channels in the retinal outer plexiform layer. Invest Ophthalmol Vis Sci *43*, 1595-1603.

Barclay, J., Balaguero, N., Mione, M., Ackerman, S. L., Letts, V. A., Brodbeck, J., Canti, C., Meir, A., Page, K. M., Kusumi, K., *et al.* (2001). Ducky mouse phenotype of epilepsy and ataxia is associated with mutations in the Cacna2d2 gene and decreased calcium channel current in cerebellar Purkinje cells. J Neurosci *21*, 6095-6104.

Benitah, J. P., Gomez, A. M., Fauconnier, J., Kerfant, B. G., Perrier, E., Vassort, G., and Richard, S. (2002). Voltage-gated Ca2+ currents in the human pathophysiologic heart: a review. Basic Res Cardiol *97 Suppl 1*, I11-18.

Berjukow, S., Marksteiner, R., Gapp, F., Sinnegger, M. J., and Hering, S. (2000). Molecular mechanism of calcium channel block by isradipine. Role of a drug-induced inactivated channel conformation. J Biol Chem *275*, 22114-22120.

Bers, D. M. (2002). Cardiac excitation-contraction coupling. Nature *415*, 198-205.

Bichet, D., Cornet, V., Geib, S., Carlier, E., Volsen, S., Hoshi, T., Mori, Y., and De Waard, M. (2000). The I-II loop of the Ca2+ channel alpha1 subunit contains an endoplasmic reticulum retention signal antagonized by the beta subunit. Neuron *25*, 177-190.

Birnbaumer, L., Qin, N., Olcese, R., Tareilus, E., Platano, D., Costantin, J., and Stefani, E. (1998). Structures and functions of calcium channel beta subunits. J Bioenerg Biomembr *30*, 357-375.

Borsotto, M., Barhanin, J., Fosset, M., and Lazdunski, M. (1985). The 1,4-dihydropyridine receptor associated with the skeletal muscle voltage-dependent Ca2+ channel. Purification and subunit composition. J Biol Chem *260*, 14255-14263.

Brice, N. L., Berrow, N. S., Campbell, V., Page, K. M., Brickley, K., Tedder, I., and Dolphin, A. C. (1997). Importance of the different beta subunits in the membrane expression of the alpha1A and alpha2 calcium channel subunits: studies using a depolarization-sensitive alpha1A antibody. Eur J Neurosci *9*, 749-759.

Cahalan, M. D., Wulff, H., and Chandy, K. G. (2001). Molecular properties and physiological roles of ion channels in the immune system. J Clin Immunol *21*, 235-252.

Canti, C., Bogdanov, Y., and Dolphin, A. C. (2000). Interaction between G proteins and accessory subunits in the regulation of 1B calcium channels in Xenopus oocytes. J Physiol *527 Pt 3*, 419-432.

Canti, C., and Dolphin, A. C. (2003). CaVbeta subunit-mediated up-regulation of CaV2.2 currents triggered by D2 dopamine receptor activation. Neuropharmacology *45*, 814-827.

Canti, C., Nieto-Rostro, M., Foucault, I., Heblich, F., Wratten, J., Richards, M. W., Hendrich, J., Douglas, L., Page, K. M., Davies, A., and Dolphin, A. C. (2005). The metal-ion-dependent adhesion site in the Von Willebrand factor-A domain of alpha2delta subunits is key to trafficking voltage-gated Ca2+ channels. Proc Natl Acad Sci U S A *102*, 11230-11235.

Carafoli, E., Santella, L., Branca, D., and Brini, M. (2001). Generation, control, and processing of cellular calcium signals. Crit Rev Biochem Mol Biol *36*, 107-260.

Catterall, W. A. (2000). Structure and regulation of voltage-gated Ca2+ channels. Annu Rev Cell Dev Biol *16*, 521-555.

Catterall, W. A., Perez-Reyes, E., Snutch, T. P., and Striessnig, J. (2005). International Union of Pharmacology. XLVIII. Nomenclature and structure-function relationships of voltage-gated calcium channels. Pharmacol Rev *57*, 411-425.

Cens, T., Restituito, S., Galas, S., and Charnet, P. (1999). Voltage and calcium use the same molecular determinants to inactivate calcium channels. J Biol Chem *274*, 5483-5490.

Chien, A. J., Carr, K. M., Shirokov, R. E., Rios, E., and Hosey, M. M. (1996). Identification of palmitoylation sites within the L-type calcium channel beta2a subunit and effects on channel function. J Biol Chem *271*, 26465-26468.

Cole, R. L., Lechner, S. M., Williams, M. E., Prodanovich, P., Bleicher, L., Varney, M. A., and Gu, G. (2005). Differential distribution of voltage-gated calcium channel alpha-2 delta (alpha2delta) subunit mRNA-containing cells in the rat central nervous system and the dorsal root ganglia. J Comp Neurol *491*, 246-269.

Colecraft, H. M., Alseikhan, B., Takahashi, S. X., Chaudhuri, D., Mittman, S., Yegnasubramanian, V., Alvania, R. S., Johns, D. C., Marban, E., and Yue, D. T. (2002). Novel functional properties of Ca(2+) channel beta subunits revealed by their expression in adult rat heart cells. J Physiol *541*, 435-452.

Curtis, B. M., and Catterall, W. A. (1984). Purification of the calcium antagonist receptor of the voltage-sensitive calcium channel from skeletal muscle transverse tubules. Biochemistry *23*, 2113-2118.

Curtis, B. M., and Catterall, W. A. (1985). Phosphorylation of the calcium antagonist receptor of the voltage-sensitive calcium channel by cAMP-dependent protein kinase. Proc Natl Acad Sci U S A *82*, 2528-2532.

Davies, A., Douglas, L., Hendrich, J., Wratten, J., Tran Van Minh, A., Foucault, I., Koch, D., Pratt, W. S., Saibil, H. R., and Dolphin, A. C. (2006). The calcium channel alpha2delta-2 subunit partitions with CaV2.1 into lipid rafts in cerebellum: implications for localization and function. J Neurosci *26*, 8748-8757.

De Jongh, K. S., Warner, C., and Catterall, W. A. (1990). Subunits of purified calcium channels. Alpha 2 and delta are encoded by the same gene. J Biol Chem *265*, 14738-14741.

de Waard, D., and Rooijers, T. (1994). An experimental study to evaluate the effectiveness of different methods and intensities of law enforcement on driving speed on motorways. Accid Anal Prev *26*, 751-765.

Dolphin, A. C. (2003). Beta subunits of voltage-gated calcium channels. J Bioenerg Biomembr *35*, 599-620.

Ellis, S. B., Williams, M. E., Ways, N. R., Brenner, R., Sharp, A. H., Leung, A. T., Campbell, K. P., McKenna, E., Koch, W. J., Hui, A., and et al. (1988). Sequence and expression of mRNAs encoding the alpha 1 and alpha 2 subunits of a DHP-sensitive calcium channel. Science *241*, 1661-1664.

Ertel, E. A., Campbell, K. P., Harpold, M. M., Hofmann, F., Mori, Y., Perez-Reyes, E., Schwartz, A., Snutch, T. P., Tanabe, T., Birnbaumer, L., *et al.* (2000). Nomenclature of voltage-gated calcium channels. Neuron *25*, 533-535.

Fatt, P., and Katz, B. (1953). The electrical properties of crustacean muscle fibres. J Physiol *120*, 171-204.

Fleig, A., and Penner, R. (1996). Silent calcium channels generate excessive tail currents and facilitation of calcium currents in rat skeletal myoballs. J Physiol *494 (Pt 1)*, 141-153.

Flockerzi, V., Oeken, H. J., Hofmann, F., Pelzer, D., Cavalie, A., and Trautwein, W. (1986). Purified dihydropyridine-binding site from skeletal muscle t-tubules is a functional calcium channel. Nature *323*, 66-68.

Gao, B., Sekido, Y., Maximov, A., Saad, M., Forgacs, E., Latif, F., Wei, M. H., Lerman, M., Lee, J. H., Perez-Reyes, E., *et al.* (2000). Functional properties of a new voltage-dependent calcium channel alpha(2)delta auxiliary subunit gene (CACNA2D2). J Biol Chem *275*, 12237-12242.

Gregg, R. G., Messing, A., Strube, C., Beurg, M., Moss, R., Behan, M., Sukhareva, M., Haynes, S., Powell, J. A., Coronado, R., and Powers, P. A. (1996). Absence of the beta subunit (cchb1) of the skeletal muscle dihydropyridine receptor alters expression of the alpha 1 subunit and eliminates excitation-contraction coupling. Proc Natl Acad Sci U S A *93*, 13961-13966.

Hagiwara, S., Ozawa, S., and Sand, O. (1975). Voltage clamp analysis of two inward current mechanisms in the egg cell membrane of a starfish. J Gen Physiol *65*, 617-644.

Hamill, O. P., Marty, A., Neher, E., Sakmann, B., and Sigworth, F. J. (1981). Improved patch-clamp techniques for high-resolution current recording from cells and cell-free membrane patches. Pflugers Arch *391*, 85-100.

He, M., Bodi, I., Mikala, G., and Schwartz, A. (1997). Motif III S5 of L-type calcium channels is involved in the dihydropyridine binding site. A combined radioligand binding and electrophysiological study. J Biol Chem *272*, 2629-2633.

Hering, S., Aczel, S., Kraus, R. L., Berjukow, S., Striessnig, J., and Timin, E. N. (1997). Molecular mechanism of use-dependent calcium channel block by phenylalkylamines: role of inactivation. Proc Natl Acad Sci U S A *94*, 13323-13328.

Hering, S., Berjukow, S., Aczel, S., and Timin, E. N. (1998). Ca2+ channel block and inactivation: common molecular determinants. Trends Pharmacol Sci *19*, 439-443.

Herlitze, S., Hockerman, G. H., Scheuer, T., and Catterall, W. A. (1997). Molecular determinants of inactivation and G protein modulation in the intracellular loop connecting domains I and II of the calcium channel alpha1A subunit. Proc Natl Acad Sci U S A *94*, 1512-1516.

Hockerman, G. H., Dilmac, N., Scheuer, T., and Catterall, W. A. (2000). Molecular determinants of diltiazem block in domains IIIS6 and IVS6 of L-type Ca(2+) channels. Mol Pharmacol *58*, 1264-1270.

Hockerman, G. H., Johnson, B. D., Abbott, M. R., Scheuer, T., and Catterall, W. A. (1997). Molecular determinants of high affinity phenylalkylamine block of L-type calcium channels in transmembrane segment IIIS6 and the pore region of the alpha1 subunit. J Biol Chem *272*, 18759-18765.

Hosey, M. M., Barhanin, J., Schmid, A., Vandaele, S., Ptasienski, J., O'Callahan, C., Cooper, C., and Lazdunski, M. (1987). Photoaffinity labelling and phosphorylation of a 165 kilodalton peptide associated with dihydropyridine and phenylalkylamine-sensitive calcium channels. Biochem Biophys Res Commun *147*, 1137-1145.

Hymel, L., Striessnig, J., Glossmann, H., and Schindler, H. (1988). Purified skeletal muscle 1,4-dihydropyridine receptor forms phosphorylation-dependent oligomeric calcium channels in planar bilayers. Proc Natl Acad Sci U S A *85*, 4290-4294.

Ivanov, S. V., Ward, J. M., Tessarollo, L., McAreavey, D., Sachdev, V., Fananapazir, L., Banks, M. K., Morris, N., Djurickovic, D., Devor-Henneman, D. E., *et al.* (2004). Cerebellar

ataxia, seizures, premature death, and cardiac abnormalities in mice with targeted disruption of the Cacna2d2 gene. Am J Pathol *165*, 1007-1018.

Jahn, H., Nastainczyk, W., Rohrkasten, A., Schneider, T., and Hofmann, F. (1988). Site-specific phosphorylation of the purified receptor for calcium-channel blockers by cAMP- and cGMP-dependent protein kinases, protein kinase C, calmodulin-dependent protein kinase II and casein kinase II. Eur J Biochem *178*, 535-542.

Jay, S. D., Sharp, A. H., Kahl, S. D., Vedvick, T. S., Harpold, M. M., and Campbell, K. P. (1991). Structural characterization of the dihydropyridine-sensitive calcium channel alpha 2-subunit and the associated delta peptides. J Biol Chem *266*, 3287-3293.

Jones, L. P., Wei, S. K., and Yue, D. T. (1998). Mechanism of auxiliary subunit modulation of neuronal alpha1E calcium channels. J Gen Physiol *112*, 125-143.

Josephson, I. R., and Varadi, G. (1996). The beta subunit increases Ca2+ currents and gating charge movements of human cardiac L-type Ca2+ channels. Biophys J *70*, 1285-1293.

Kang, M. G., and Campbell, K. P. (2003). Gamma subunit of voltage-activated calcium channels. J Biol Chem *278*, 21315-21318.

Klockner, U., Mikala, G., Schwartz, A., and Varadi, G. (1996). Molecular studies of the asymmetric pore structure of the human cardiac voltage- dependent Ca2+ channel. Conserved residue, Glu-1086, regulates proton-dependent ion permeation. J Biol Chem *271*, 22293-22296.

Koch, S. E., Bodi, I., Schwartz, A., and Varadi, G. (2000). Architecture of Ca(2+) channel pore-lining segments revealed by covalent modification of substituted cysteines. J Biol Chem *275*, 34493-34500.

Lacinova, L., Ludwig, A., Bosse, E., Flockerzi, V., and Hofmann, F. (1995). The block of the expressed L-type calcium channel is modulated by the beta 3 subunit. FEBS Lett *373*, 103-107.

Leung, A. T., Imagawa, T., and Campbell, K. P. (1987). Structural characterization of the 1,4-dihydropyridine receptor of the voltage-dependent Ca2+ channel from rabbit skeletal muscle. Evidence for two distinct high molecular weight subunits. J Biol Chem *262*, 7943-7946.

Li, C. Y., Song, Y. H., Higuera, E. S., and Luo, Z. D. (2004). Spinal dorsal horn calcium channel alpha2delta-1 subunit upregulation contributes to peripheral nerve injury-induced tactile allodynia. J Neurosci *24*, 8494-8499.

Li, C. Y., Zhang, X. L., Matthews, E. A., Li, K. W., Kurwa, A., Boroujerdi, A., Gross, J., Gold, M. S., Dickenson, A. H., Feng, G., and Luo, Z. D. (2006). Calcium channel alpha2delta1 subunit mediates spinal hyperexcitability in pain modulation. Pain *125*, 20-34.

Luo, Z. D., Calcutt, N. A., Higuera, E. S., Valder, C. R., Song, Y. H., Svensson, C. I., and Myers, R. R. (2002). Injury type-specific calcium channel alpha 2 delta-1 subunit up-regulation in rat neuropathic pain models correlates with antiallodynic effects of gabapentin. J Pharmacol Exp Ther *303*, 1199-1205.

Luo, Z. D., Chaplan, S. R., Higuera, E. S., Sorkin, L. S., Stauderman, K. A., Williams, M. E., and Yaksh, T. L. (2001). Upregulation of dorsal root ganglion (alpha)2(delta) calcium channel subunit and its correlation with allodynia in spinal nerve-injured rats. J Neurosci *21*, 1868-1875.

Marais, E., Klugbauer, N., and Hofmann, F. (2001). Calcium channel alpha(2)delta subunits-structure and Gabapentin binding. Mol Pharmacol *59*, 1243-1248.

Mathias, R. T., Cohen, I. S., and Oliva, C. (1990). Limitations of the whole cell patch clamp technique in the control of intracellular concentrations. Biophys J *58*, 759-770.

Meier, H. (1968). The neuropathology of ducky, a neurological mutation of the mouse. A pathological and preliminary histochemical study. Acta Neuropathol *11*, 15-28.

Meir, A., and Dolphin, A. C. (2002). Kinetics and Gbetagamma modulation of Ca(v)2.2 channels with different auxiliary beta subunits. Pflugers Arch *444*, 263-275.

Mikala, G., Bahinski, A., Yatani, A., Tang, S., and Schwartz, A. (1993). Differential contribution by conserved glutamate residues to an ion-selectivity site in the L-type Ca2+ channel pore. FEBS Lett *335*, 265-269.

Motoike, H. K., Bodi, I., Nakayama, H., Schwartz, A., and Varadi, G. (1999). A region in IVS5 of the human cardiac L-type calcium channel is required for the use-dependent block by phenylalkylamines and benzothiazepines. J Biol Chem *274*, 9409-9420.

Murakami, M., Yamamura, H., Murakami, A., Okamura, T., Nunoki, K., Mitui-Saito, M., Muraki, K., Hano, T., Imaizumi, Y., Flockerzi, T., and Yanagisawa, T. (2000). Conserved smooth muscle contractility and blood pressure increase in response to high-salt diet in mice lacking the beta3 subunit of the voltage-dependent calcium channel. J Cardiovasc Pharmacol *36 Suppl 2*, S69-73.

Nastainczyk, W., Rohrkasten, A., Sieber, M., Rudolph, C., Schachtele, C., Marme, D., and Hofmann, F. (1987). Phosphorylation of the purified receptor for calcium channel blockers by cAMP kinase and protein kinase C. Eur J Biochem *169*, 137-142.

Neely, A., Wei, X., Olcese, R., Birnbaumer, L., and Stefani, E. (1993). Potentiation by the beta subunit of the ratio of the ionic current to the charge movement in the cardiac calcium channel. Science *262*, 575-578.

Newton, R. A., Bingham, S., Case, P. C., Sanger, G. J., and Lawson, S. N. (2001). Dorsal root ganglion neurons show increased expression of the calcium channel alpha2delta-1 subunit following partial sciatic nerve injury. Brain Res Mol Brain Res *95*, 1-8.

Nilius, B., Hess, P., Lansman, J. B., and Tsien, R. W. (1985). A novel type of cardiac calcium channel in ventricular cells. Nature *316*, 443-446.

Nowycky, M. C., Fox, A. P., and Tsien, R. W. (1985). Three types of neuronal calcium channel with different calcium agonist sensitivity. Nature *316*, 440-443.

O'Callahan, C. M., Ptasienski, J., and Hosey, M. M. (1988). Phosphorylation of the 165-kDa dihydropyridine/phenylalkylamine receptor from skeletal muscle by protein kinase C. J Biol Chem *263*, 17342-17349.

Olcese, R., Neely, A., Qin, N., Wei, X., Birnbaumer, L., and Stefani, E. (1996). Coupling between charge movement and pore opening in vertebrate neuronal alpha 1E calcium channels. J Physiol *497 (Pt 3)*, 675-686.

Olcese, R., Qin, N., Schneider, T., Neely, A., Wei, X., Stefani, E., and Birnbaumer, L. (1994). The amino terminus of a calcium channel beta subunit sets rates of channel inactivation independently of the subunit's effect on activation. Neuron *13*, 1433-1438.

Opatowsky, Y., Chomsky-Hecht, O., Kang, M. G., Campbell, K. P., and Hirsch, J. A. (2003). The voltage-dependent calcium channel beta subunit contains two stable interacting domains. J Biol Chem *278*, 52323-52332.

Perez-Reyes, E. (2003). Molecular physiology of low-voltage-activated t-type calcium channels. Physiol Rev *83*, 117-161.

Pragnell, M., De Waard, M., Mori, Y., Tanabe, T., Snutch, T. P., and Campbell, K. P. (1994). Calcium channel beta-subunit binds to a conserved motif in the I-II cytoplasmic linker of the alpha 1-subunit. Nature *368*, 67-70.

Qin, N., Platano, D., Olcese, R., Costantin, J. L., Stefani, E., and Birnbaumer, L. (1998). Unique regulatory properties of the type 2a Ca2+ channel beta subunit caused by palmitoylation. Proc Natl Acad Sci U S A *95*, 4690-4695.

Qin, N., Yagel, S., Momplaisir, M. L., Codd, E. E., and D'Andrea, M. R. (2002). Molecular cloning and characterization of the human voltage-gated calcium channel alpha(2)delta-4 subunit. Mol Pharmacol *62*, 485-496.

Raghib, A., Bertaso, F., Davies, A., Page, K. M., Meir, A., Bogdanov, Y., and Dolphin, A. C. (2001). Dominant-negative synthesis suppression of voltage-gated calcium channel Cav2.2 induced by truncated constructs. J Neurosci *21*, 8495-8504.

Reuter, H. (1967). The dependence of slow inward current in Purkinje fibres on the extracellular calcium-concentration. J Physiol *192*, 479-492.

Reuter, H., Stevens, C. F., Tsien, R. W., and Yellen, G. (1982). Properties of single calcium channels in cardiac cell culture. Nature *297*, 501-504.

Rohrkasten, A., Meyer, H. E., Nastainczyk, W., Sieber, M., and Hofmann, F. (1988). cAMP-dependent protein kinase rapidly phosphorylates serine- 687 of the skeletal muscle receptor for calcium channel blockers. J Biol Chem *263*, 15325-15329.

Rotman, E. I., De Jongh, K. S., Florio, V., Lai, Y., and Catterall, W. A. (1992). Specific phosphorylation of a COOH-terminal site on the full-length form of the alpha 1 subunit of the skeletal muscle calcium channel by cAMP-dependent protein kinase. J Biol Chem *267*, 16100-16105.

Rotman, E. I., Murphy, B. J., and Catterall, W. A. (1995). Sites of selective cAMP-dependent phosphorylation of the L-type calcium channel alpha 1 subunit from intact rabbit skeletal muscle myotubes. J Biol Chem *270*, 16371-16377.

Ruth, P., Rohrkasten, A., Biel, M., Bosse, E., Regulla, S., Meyer, H. E., Flockerzi, V., and Hofmann, F. (1989). Primary structure of the beta subunit of the DHP-sensitive calcium channel from skeletal muscle. Science *245*, 1115-1118.

Schmid, A., Renaud, J. F., and Lazdunski, M. (1985). Short term and long term effects of beta-adrenergic effectors and cyclic AMP on nitrendipine-sensitive voltage-dependent Ca2+ channels of skeletal muscle. J Biol Chem *260*, 13041-13046.

Sculptoreanu, A., Scheuer, T., and Catterall, W. A. (1993). Voltage-dependent potentiation of L-type Ca2+ channels due to phosphorylation by cAMP-dependent protein kinase. Nature *364*, 240-243.

Sharp, A. H., and Campbell, K. P. (1989). Characterization of the 1,4-dihydropyridine receptor using subunit-specific polyclonal antibodies. Evidence for a 32,000-Da subunit. J Biol Chem *264*, 2816-2825.

Shistik, E., Ivanina, T., Puri, T., Hosey, M., and Dascal, N. (1995). Ca2+ current enhancement by alpha 2/delta and beta subunits in Xenopus oocytes: contribution of changes in channel gating and alpha 1 protein level. J Physiol *489 (Pt 1)*, 55-62.

Sieber, M., Nastainczyk, W., Zubor, V., Wernet, W., and Hofmann, F. (1987). The 165-kDa peptide of the purified skeletal muscle dihydropyridine receptor contains the known regulatory sites of the calcium channel. Eur J Biochem *167*, 117-122.

Spaetgens, R. L., and Zamponi, G. W. (1999). Multiple structural domains contribute to voltage-dependent inactivation of rat brain alpha(1E) calcium channels. J Biol Chem *274*, 22428-22436.

Striessnig, J., Murphy, B. J., and Catterall, W. A. (1991). Dihydropyridine receptor of L-type Ca2+ channels: identification of binding domains for [3H](+)-PN200-110 and [3H]azidopine within the alpha 1 subunit. Proc Natl Acad Sci U S A *88*, 10769-10773.

Sutton, K. G., Martin, D. J., Pinnock, R. D., Lee, K., and Scott, R. H. (2002). Gabapentin inhibits high-threshold calcium channel currents in cultured rat dorsal root ganglion neurones. Br J Pharmacol *135*, 257-265.

Takahashi, M., and Catterall, W. A. (1987). Dihydropyridine-sensitive calcium channels in cardiac and skeletal muscle membranes: studies with antibodies against the alpha subunits. Biochemistry *26*, 5518-5526.

Takahashi, M., Narisawa, T., Masuda, T., Nagasawa, O., Suzuki, K., Yoshioka, H., and Koyama, H. (1987a). [Inhibition of the growth of a murine transplantable tumor, colon 26, by the prostaglandin synthetase inhibitor, indomethacin]. Gan To Kagaku Ryoho *14*, 2334-2340.

Takahashi, M., Seagar, M. J., Jones, J. F., Reber, B. F., and Catterall, W. A. (1987b). Subunit structure of dihydropyridine-sensitive calcium channels from skeletal muscle. Proc Natl Acad Sci U S A *84*, 5478-5482.

Takahashi, S. X., Mittman, S., and Colecraft, H. M. (2003). Distinctive modulatory effects of five human auxiliary beta2 subunit splice variants on L-type calcium channel gating. Biophys J *84*, 3007-3021.

Tanabe, T., Takeshima, H., Mikami, A., Flockerzi, V., Takahashi, H., Kangawa, K., Kojima, M., Matsuo, H., Hirose, T., and Numa, S. (1987). Primary structure of the receptor for calcium channel blockers from skeletal muscle. Nature *328*, 313-318.

Triggle, D. J. (2007). Calcium channel antagonists: clinical uses—past, present and future. Biochem Pharmacol *74*, 1-9.

Vaghy, P. L., Striessnig, J., Miwa, K., Knaus, H. G., Itagaki, K., McKenna, E., Glossmann, H., and Schwartz, A. (1987). Identification of a novel 1,4-dihydropyridine- and phenylalkylamine-binding polypeptide in calcium channel preparations. J Biol Chem *262*, 14337-14342.

Viard, P., Butcher, A. J., Halet, G., Davies, A., Nurnberg, B., Heblich, F., and Dolphin, A. C. (2004). PI3K promotes voltage-dependent calcium channel trafficking to the plasma membrane. Nat Neurosci *7*, 939-946.

Wang, H., Sun, H., Della Penna, K., Benz, R. J., Xu, J., Gerhold, D. L., Holder, D. J., and Koblan, K. S. (2002). Chronic neuropathic pain is accompanied by global changes in gene

expression and shares pathobiology with neurodegenerative diseases. Neuroscience *114*, 529-546.

Yamaguchi, H., Hara, M., Strobeck, M., Fukasawa, K., Schwartz, A., and Varadi, G. (1998). Multiple modulation pathways of calcium channel activity by a beta subunit. Direct evidence of beta subunit participation in membrane trafficking of the alpha1C subunit. J Biol Chem *273*, 19348-19356.

Zamponi, G. W., Soong, T. W., Bourinet, E., and Snutch, T. P. (1996). Beta subunit coexpression and the alpha1 subunit domain I-II linker affect piperidine block of neuronal calcium channels. J Neurosci *16*, 2430-2443.

Zhang, J. F., Ellinor, P. T., Aldrich, R. W., and Tsien, R. W. (1994). Molecular determinants of voltage-dependent inactivation in calcium channels. Nature *372*, 97-100.

2 CHAPTER II

INTERACTION OF DILTIAZEM BY WITH AN INTRACELLULAR ACCESSABLE BINDING SITE ON CA_V 1.2

Published as Shabbier et al. in BJP 2011 Mar;162(5):1074-82.

2.1 INTRODUCTION

L-type calcium channels belong to the high-voltage activated channel family (isoforms $Ca_V1.1$, $Ca_V1.2$, $Ca_V1.3$ and $Ca_V1.4$) and display a high sensitivity to calcium channel blockers (or Ca^{2+} antagonists) (Catterall et al., 2005). $Ca_V1.2$ participates in excitation-contraction coupling in cardiac and smooth muscle, action potential propagation in sinoatrial and atrioventricular node, synaptic plasticity and hormone secretion and other processes (Striessnig et al., 1999; Catterall et al., 2000, Schulla et al., 2003, Sinnegger-Brauns et al., 2004). Calcium antagonists are widely used to treat cardiovascular diseases such as hypertension, angina pectoris and arrhythmias (Triggle, 2007, Striessnig et al., 1999). They are a chemically heterogeneous group of drugs that exert their therapeutic effects by inhibiting voltage-gated L-type Ca^{2+} channels. The prototypical agents of this group are diltiazem (Dil; a benzothiazepinone, BTZ), nifedipine (a 1,4-dihydropyridine, DHP) and verapamil (a phenylalkylamine, PAA). Single amino acids determining the sensitivity of L-type channels for calcium antagonists have been identified by mutational analysis and functional studies (Hering et al., 1996, Kraus et al., 1998, Striessnig et al, 1998, Berjukow et al., 1999 Hockerman et al., 2000, Dilmac et al., 2003).

The binding sites for PAA and diltiazem share common amino acid residues but it is assumed that the two drug classes access their binding pockets from different sides of the membrane. There is clear evidence from studies with quaternary PAA analogues applied via the patch pipette that this class of $Ca_V1.2$ inhibitors interacts with an intracellular located binding site (Hescheler et al., 1982; Berjukov et al., 1996). Thus it is widely believed that tertiary PAAs penetrate the membrane and block $Ca_V1.2$ from the cytosolic side of the membrane in their protonated form in a use-dependent manner. $Ca_V1.2$ inhibition by diltiazem is also use-dependent (Lee and Tsien, 1983; Uehara and Hume, 1985; Smirnov and Aaronson, 1998). Variation of external and internal pH revealed that diltiazem inhibits L-type channels in its

charged and neutral forms (Smirnov and Aaronson, 1998). Studies with a structurally related benzothiazepine (SQ32,428) suggested, however, an extracellular location of the diltiazem binding site (Hering et al., 1993). The latter finding is in apparent contradiction with mutational studies indicating that crucial diltiazem binding determinants overlap with determinants of PAA sensitivity located deeply in the channel pore (Hering et al., 1996; Kraus et al., 1998; Burjokow et al., 1999; Hockerman et al., 2000; Dilmac et al., 2003). Tikhonov and Zhorov (2008) pointed out that the potential BTZ binding determinants are located in the inner pore of Cav1.2 while some quaternary BTZ block the channel when applied externally rather than internally. The authors proposed a molecular model explaining the interaction with key amino acids of the putative binding pocket that were identified in functional studies. Tikhonov and Zhorov (2008) suggest that drug access occurs via the III/IV domain interface from the outside of the membrane.

However, to date no study has systematically examined the extracellular and intracellular action of the therapeutically used diltiazem on $Ca_V1.2$. Therefore we synthesised the quaternary derivative of d-cis-diltiazem, qDil, and explored its effects when applied from outside or inside (via the patch pipette) of the cell membrane. Our data on wild-type and mutant $Ca_V1.2$ clearly demonstrate “use-dependent” intracellular access of qDil to the diltiazem binding pocket in $Ca_V1.2$.

2.2 METHODS

2.2.1 *General Experimental Methods*

All chemicals obtained from commercial suppliers were used as received and were of analytical grade. Melting points were determined on a Kofler hot stage apparatus and are uncorrected. The ^{1}H- and ^{13}C-NMR spectra were recorded on a Bruker Avance DPx200 (200 and 50 MHz).

2.2.2 Synthesis of quaternary Diltiazem

To a solution of the free base of 0,829g (2 mmol) Diltiazem in 2 ml dichloromethane 0,568g (4 mmol) of iodomethane were added at room temperature. After 48h the reaction mixture was concentrated to dryness. The crude product of qDil was obtained and recrystallized from isopropanol to yield 0,807g (97 %) of qDil.

The analysis of this material gave the following results: Mp 178-181°C; ^{1}H-NMR (D_2O): δ 7.68 -7.64 (m, 3H), δ 7.38-7.26 (m, 3H), δ 6.89 ($J_{A,B}$=8.58 Hz, 2H), δ 5.04 (q, 2H), δ 4.13-4.08 (m, 1H), δ 3.96-3.83 (m, 2H), δ 3.72 (s, 4H), δ 3.42-3.38 (m, 1H), δ 3.09 (s, 9H), δ 1.80 (s, 3H); ^{13}C-NMR (D_2O): δ 170.29, δ 169.10, δ 160.28, δ 144.35, δ 136.24, δ 132.83, δ 131.02, δ 128.92, δ 127.65, δ 126.32, δ 125.63, δ 114.36, δ 71.85, δ 63.47, δ 55.74, δ 54.61, δ 50.10, δ 44.54, δ 20,89.

2.2.3 Purity of qDil

The purity of qDil was confirmed by HPLC and was 98%. The analysis was performed using a Jasco UV-1575 Chromatograph. The stationary phase was a 5µm RP-18e Lichrospher Merck column (250mm x 4mm). As a mobile phase, ammonium acetate pH 6.0 + 0,5% DEA/CAN (50/50) was used.

2.2.4 Cell Culture and Transient Transfection

Human embryonic kidney tsA-201 cells were grown at 5% CO2 and 37°C to 80% confluence in Dulbecco's modified Eagle's medium/F-12 supplemented with 10% (v/v) fetal calf serum and 100 units/ml of penicillin and streptomycin. Cells were split using trypsin/EDTA and plated on 35-mm Petri dishes (Falcon) at 30-50% confluence 16 h before transfection. Subsequently, tsA-201 cells were co-transfected with cDNAs encoding wild-type (GenBankTM accession number X15539) or mutant $Ca_V1.2$ α1-subunits (I1150A, I1153A, I1156A, M1160A, F1164A, V1165A, I1460A, I1464A, Y1463F, F1117G, E1118Q, E1419Q; Hockermann et al., 2000) with auxiliary β_{2a}, $\alpha_2\delta$ subunits (Ellis et al., 1998). The transfection

of tsA-201 cells was performed using the FuGENE 6 transfection reagent (Roche Applied Science) following standard protocols.

2.2.5 Ionic Current Recordings and Data Acquisition

Barium currents (I_{Ba}) through voltage-gated Ca^{2+} channels were recorded at 22-25°C using the whole cell patch-clamp configration (Hamill et al., 1981) by Axopatch 200A patch clamp amplifier (Axon Instruments) 36-48 h after transfection.The extracellular bath solution contained 20 mM $BaCl_2$, 1 mM $MgCl_2$, 10 mM HEPES, and 140 mM choline-Cl, titrated to pH 7.4 with methanesulfonic acid. The borosilicate glass patch pipettes (HARVARD APPARATUS) with resistances of 1–4 megohms were pulled and polished using a DMZ universal puller (Zeiss instruments, Germany), and were filled with pipette solution containing 145 mM CsCl, 3 mM $MgCl_2$, 10 mM HEPES, and 10 mM EGTA, titrated to pH 7.25 with CsOH.

Intracellular application was done via the patch pipettes and I_{Ba} were recorded 5 min after the whole cell configuration was established. To ensure that the internal drug concentration reached steady state, use-dependent block was monitored after different time intervals. An approximation of the time for intracellular perfusion (Mathias et al., 1990) predicts that under our experimental conditions, an equilibrium between the pipette concentration of qDil and the intracellular solution should be reached within about 10 s.

For extracellular application, the drug was applied to cells under voltage clamp using a microminifold perfusion system (ALA scientific Instruments, Westbury, NY). I_{Ba} were recorded by applying repetitive pulses after a 5 min equilibration period in drug-containing solution. Use-dependent Ca^{2+} channel block was estimated as peak I_{Ba} inhibition during a train of short (100 ms) test pulses from -80 mV at a frequency of 0.2 Hz. The dose-response curves of I_{Ba} inhibition were fitted using the Hill equation, $\frac{I_{Ba,drug}}{I_{Ba,control}}(in\%) = \frac{100 - A}{1 + \left(\frac{C}{IC_{50}}\right)^{nH}} + B$,

where IC_{50} is the concentration at which I_{Ba} inhibition is half-maximal, C is the applied drug

concentration, B represents a non-blocked current and A the blocked current fraction (both in percent). Channel block levels observed in the presence of drug were corrected by subtracting the mean steady state inhibition (after 20 pulses, see Table 1) in controls. All data were digitized using a DIGIDATA 1200 interface (Axon Instruments), smoothed by means of a four-pole Bessel filter, and stored on computer hard disc. Leak currents were subtracted digitally using average values of scaled leakage currents elicited by a 10 mV hyperpolarizing pulse. Series resistance and offset voltage were routinely compensated. The pClamp software package (version 7.0 Axon Instruments, Inc.) was used for data acquisition and preliminary analysis.

The voltage-dependence of activation was determined from current-voltage (I-V) curves in the absence and presence of drug. The curves were fitted according to the following modified Boltzmann term:

$$I = \frac{G_{\max} \cdot (V - V_{rev})}{1 + \exp \frac{V_{0.5,act} - V}{k_{act}}}$$

where V_{rev}, extrapolated reversal potential; V, membrane potential; I, peak current; G_{max}, maximum membrane conductance; $V_{0.5,\ act}$' voltage for half-maximal activation; and k_{act}, slope factor.

The voltage-dependence of I_{Ba} inactivation (inactivation curve) in the presence and absence of drug was measured using a multi-step protocol (see Hohaus et al. 2005). In order to avoid accumulation of channel block, the pulse sequence was applied every 2 minutes from a holding potential of -80 mV. Inactivation curves were drawn according to a Boltzmann equation:

$$I_{Ba,inactivation} = I_{SS} + \frac{1 - I_{SS}}{1 + \exp \frac{V - V_{0.5,inact}}{k_{inact}}}$$

where V, membrane potential; $V_{0.5,\ inact}$, midpoint voltage; $k_{\ inact}$, slope factor and I_{ss}, fraction of non-inactivating current.

Recovery from block was monitored by applying 6 short (20 ms) test pulses after the conditioning train. Application of the monitoring pulses in the presence of 300 µM of the used drugs did not induce measurable channel inhibition.

Analysis and curve fitting was done with Microcal Origin 7.0. Data are given as Mean±S.E. Statistical significance was assessed using the Student's unpaired t-test.

2.3 RESULTS

To clarify the interaction of diltiazem with either an extra- or intracellular binding site on $Ca_V1.2$, the membrane-impermeable quaternary derivative of d-cis-diltiazem (qDil) was synthesized (see Methods). $Ca_V1.2$ composed of wild-type or mutant α1 subunits and auxiliary α2-δ and β2a subunits were expressed in tsA 201 cells. qDil was applied intracellularly via the patch pipette and extracellularly in the perfusion bath.

2.3.1 Intracellular and extracellular effects of quaternary d-cis-diltiazem

As shown in Fig. 1 A qDil blocks I_{Ba} in a "use dependent" manner when applied via the patch pipette. I_{Ba} inhibition was induced by applying a train of 100 ms test pulses from -80 to 20 mV at a frequency of 0.2 Hz. Fig. 1 C, D illustrates the acceleration of the current decay (statically not significant)

during the first pulse. Current traces from control cells and first pulse currents of a train with qDil in the pipette were normalized and averaged. The direct comparison of control I_{Ba} and I_{Ba} in drug was not possible under these conditions.

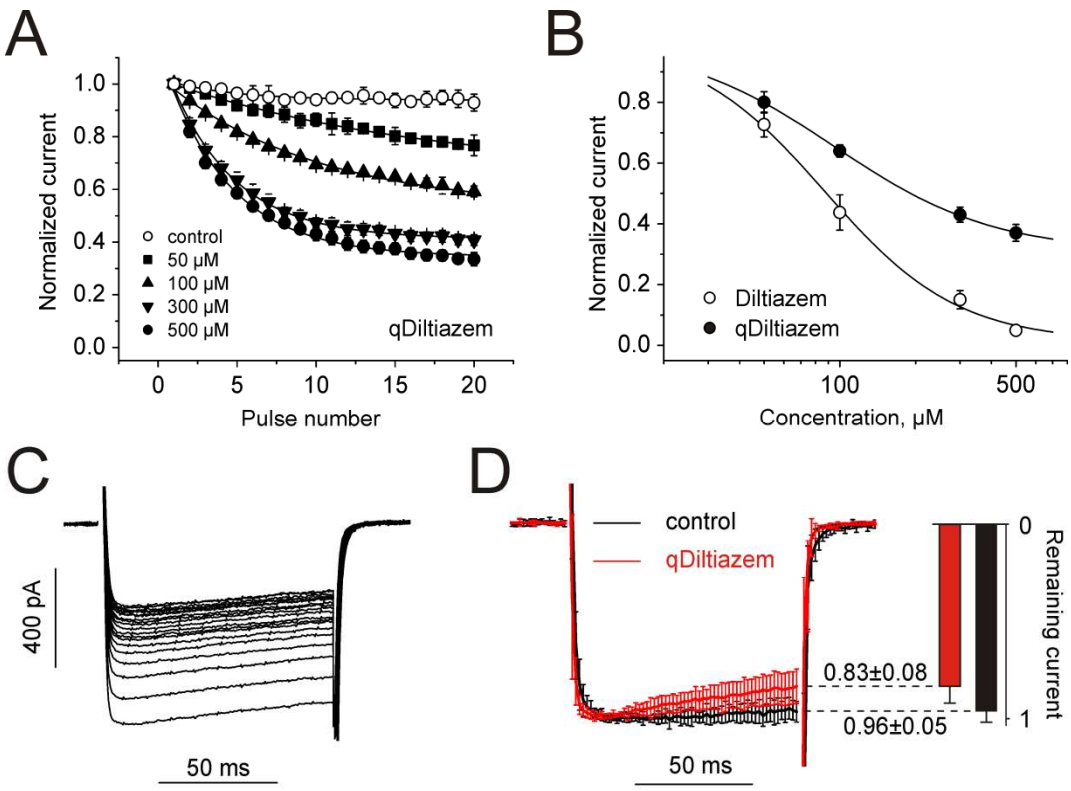

Fig. 1 Use-dependent block of $Ca_V1.2$ by intracellularly applied quaternary diltiazem.

A, Use-dependent inhibition of wild-type channels measured in the absence or presence of 50, 100, 300 or 500 µM quaternary diltiazem in the intracellular (pipette) solution. Data points are the mean from 4-6 experiments.

B, The IC50 values (d-cis-diltiazem: 95±5 µM (Hill slope n_H=1.6±0.4) and qDil: 85±9 µM (n_H=1.3±0.2)) were obtained by fitting the data points to the Hill equation (as described in "Methods" section). Channel block was estimated as peak I_{Ba} inhibition during trains of 20 pulses (0.2 Hz, 100 ms) applied from a holding potential of -80 mV to +20 mV in control (Table 1) and in presence of quaternary diltiazem.

C, Superimposed I_{Ba} during a train of 20 pulses with 300 µM quaternary diltiazem in pipette.

D, Acceleration of current decay during the first pulse in train. Current traces were normalized and averaged. The mean peak current densities were -14.7 ± 0.9 (control) and -13.8 ± 0.9 pA/pF (first pulse current after 3 minutes 300 µM qDil in the pipette). Bar graphs indicate remaining current at the end of the first pulse.

Table 1 Peak current decay in the absence of drug after 20 pulses (100 ms) at 0.2 Hz

Mutation	Control inhibition, %
WT	5.9±3.0
I1150A	3.6±1.5
I1153A	9.9±2.1
I1156A	9.3±1.8
M1160A	14.8±1.6
F1164A	10.1±3.3
V1165A	0.7±1.8
I1460A	10.6±0.9
Y1463F	0.9±1.2
M1464A	0.7±3.0
F1117G	9.5±1.2
E1118Q	9.2±1.8
E1419Q	3.6±4.8

In order to evaluate potential resting state inhibition by qDil from the intracellular side we compared the peak current densities in control and after 3 minutes intracellular application of qDil (300 µM). The mean peak current densities of -14.7 ± 0.9 (control) and -13.8 ± 0.9 pA/pF (calculated from first pulse I_{Ba} with 300 µM qDil in the pipette) suggest that qDil when applied from the intracellular side of the membrane induces only non significant resting state inhibition. We can not exclude that the reduced peak current density reflects open channel inhibition developing during the rising phase of current.

The kinetics of peak current inhibition during pulse trains and the final steady state values were dependent on qDil concentration. The steady state values plotted versus the applied drug

concentrations are shown in Fig. 1 B. The IC_{50} values for I_{Ba} inhibition of wild-type $Ca_V1.2$ by qDil and Dil were 95±5 µM and 85±9 µM respectively (Fig. 1 B).

Extracellular application of 300 µM qDil induced 10±4% use-dependent I_{Ba} inhibition of wild-type $Ca_V1.2$ (Fig. 2 A,B) which was statistically not significantly different from the current decay during a pulse train in the absence of drug (6±3%). The same drug concentration induced 59±4% I_{Ba} inhibition when applied via the pipette indicating that qDil accesses its binding site on $Ca_V1.2$ from the intracellular side of the membrane (Fig. 1B).

The tonic block of I_{Ba} (current inhibition after 3 min in drug at rest) induced by 100 and 300 µM Dil and qDil is shown in Fig. 2 D. Neither 100 nor 300 µM of qDil induced substantial I_{Ba} inhibition (12±2% and 16±2% respectively). This block was not enhanced by repetitive pulsing. Extracellularly applied Dil induced larger tonic current inhibition than qDil which can be prescribed to channel inhibition by the neutral form of the drug (see Smirnov and Aaronson, 1998).

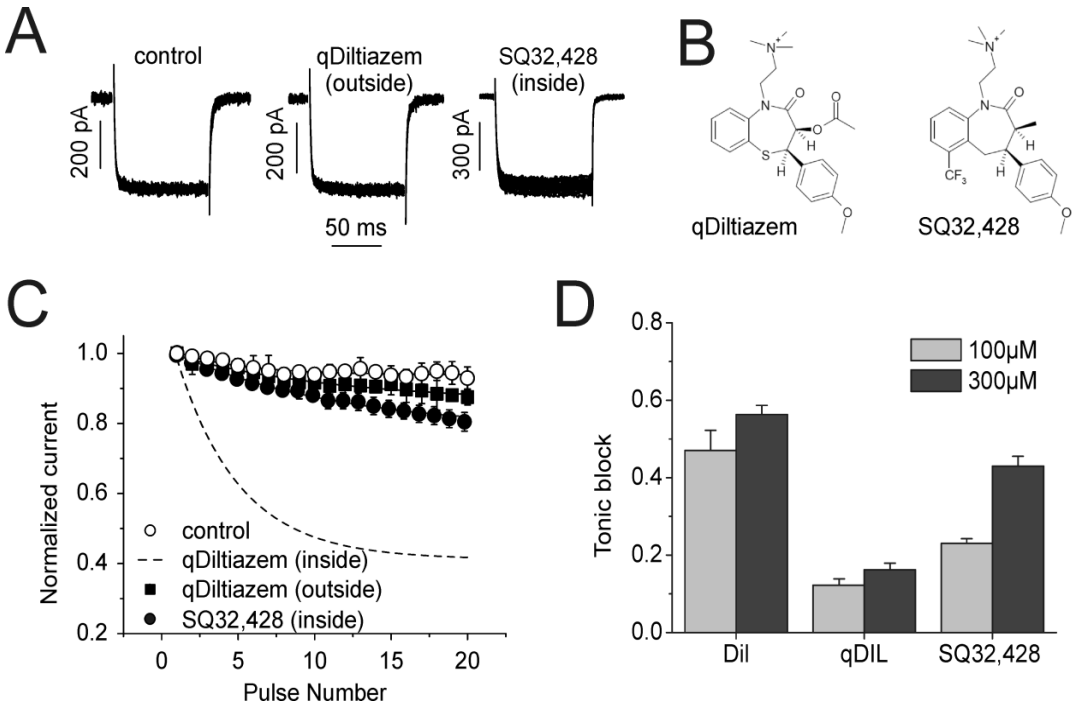

Fig. 2 Extracellular quaternary diltiazem and intracellular SQ32,428 do not inhibit $Ca_V1.2$.

A. Superimposed I_{Ba} during a train of 20 pulses (same protocol as in Fig. 1) in the absence of drug, with 300 µM quaternary diltiazem in the bath solution and with 300 µM SQ32,428 in pipette.

B, Structures of quaternary diltiazem and BTZ SQ32,428.

C, Lack of significant I_{Ba} inhibition by extracellularly applied qDil (300 µM) and intracellularly applied SQ32,428 (300 µM). Peak current decay with 300 µM qDil in the pipette is shown for comparison as a broken line (data from Fig. 1A). Data points are the mean from 4-6 experiments.

D, Bar graphs illustrate tonic I_{Ba} inhibition (block after 3 minutes in drug at rest at -80 mV) induced by 100 and 300 µM Dil, qDil and SQ32,428 applied extracellularly.

Intracellularly applied 300 µM SQ 32,428 (a quaternary benzothiazepine, see also Hering et al., 1993) induce minor channel inhibition (Fig. 2 C). The structures of qDil and SQ 32,428 are compared in Fig. 2 B. Externally applied SQ 32,428 (100 and 300 µM) inhibited I_{Ba} by 23±2% (n=5) and 43±3% (n=5) in a non use-dependent manner (Fig. 2 D, see Hering et al., 1993 for similar experiments on BC3H1 cells).

In order to estimate potential tonic inhibition by qDil applied via the patch pipette we compared the currents in control (pipette does not contain qDil) with the first pulse I_{Ba} amplitude after a 3 minute equilibration with 300 µM qDil in the pipette. The estimated current densities of -14.7±0.9 pA/pF and -13.8 ±0.9 pA/pF suggest that qDil induces non significant resting state inhibition when applied from the intracellular side of the membrane.

2.3.2 qDil interaction with the diltiazem binding site

Six amino acid residues on segment IIIS6 and three residues on segment IVS6 (Fig. 3 A) of the $Ca_V1.2$ α1 subunit have been shown to affect channel inhibition by Dil (Hering et al., 1996; Hockerman et al., 2000; Dilmac et al., 2003). To elucidate whether its quaternary

derivative interacts with the same binding pocket we first studied I_{Ba} inhibition in IIIS6 mutants I1150A, I1153A, I1156A, M1160A, F1164A and V1165A by intracellularly applied qDil. Three mutants (I1150A, F1164A, V1165A) significantly reduced sensitivity for qDil (Fig. 3 B, C) which is in line with their strong effects on Dil sensitivity (Hockerman et al. 2000). The other mutations induced moderate (not statistically significant) effects which might reflect the different experimental conditions. Rare pulsing every 20 sec (0.05 Hz) from -60 mV induces predominantly tonic block (Hockerman et al. 2000) while frequent pulsing every 5 sec (0.2 Hz) induces predominantly use-dependent block (present study). Mutations of the key determinants of Dil sensitivity in segment IVS6 (I1460A, Y1463F and M1464A, Hockerman et al. 2000) all significantly reduced qDil sensitivity (Fig. 3 D, E). To determine a possible interaction of qDil with potential binding sites in the selectivity filter we analyzed I_{Ba} inhibition of mutants F1117G, E1118Q and E1419Q. A moderate reduction in block compared to wild type was observed (Fig 3 F, G) which is in line with a study of Dilmac et al. (2003).

A

IIIS6 ISIFF**I**IY**I**II**I**AFF**M**MNI**FV**AL (1145-1167)
IVS6 AVFYF**I**SF**YM**LCAFLIINLFVAV (1455-1477)

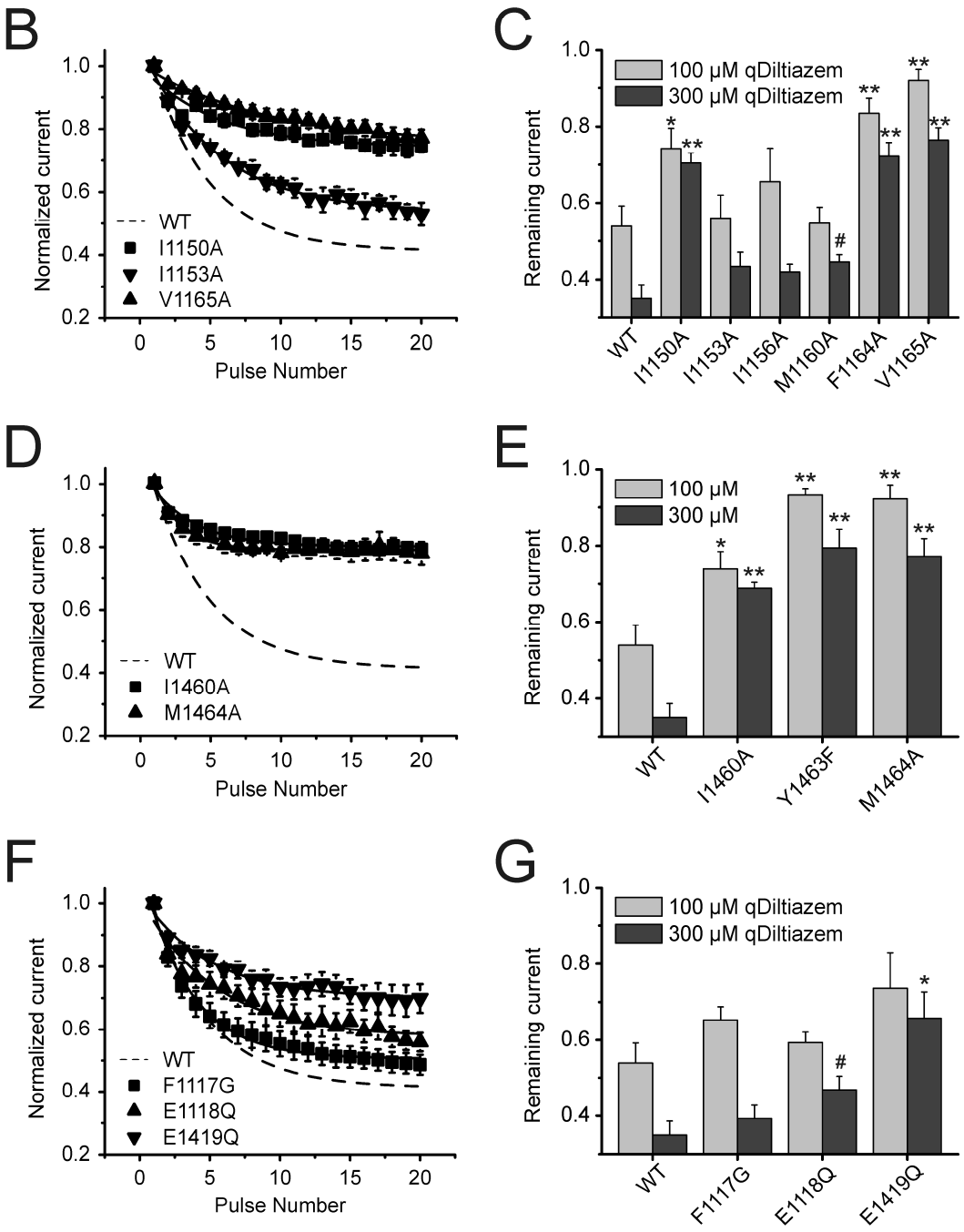

Fig. 3 Mutations of the putative Dil binding site affect I_{Ba} inhibition by intracellularly applied qDil.

A, Amino acid sequence of the transmembrane segments IIIS6 and IVS6 of the $Ca_V1.2$ α_1 subunit. Putative diltiazem binding determinants are highlighted.

B, Peak current decay in mutants I1150A, I1153A, and V1165A channels induced by 300 μM quaternary diltiazem in the pipette solution (protocol as in Fig. 1).

C, Remaining currents after 20 pulses in WT and the indicated IIIS6 mutants. Asterisks denote that the steady state block value for quaternary diltiazem of the indicated mutant channel is significantly different from that of WT (Student's *t* test: $*P < 0.05$, $**P < 0.01$, $^{\#}P = 0.057$).

D, Use-dependent inhibition of I460A and M1464A channels by 300 μM of qDil in the pipette solution.

E, Remaining currents of WT $Ca_V1.2$ and the indicated IVS6 mutants. Asterisks indicate that the steady state block value for quaternary diltiazem of the indicated mutant channel is significantly different from that of WT (Student's *t* test: $*p < 0.05$, $**p < 0.01$).

F, Use-dependent inhibition of selectivity filter mutants F1117G, E1118Q and E1419Q by 300 μM qDil in the pipette solution.

G, Remaining currents after 20 pulses in WT and the indicated $Ca_V1.2$ mutants in 100 and 300 μM qDil in the pipette. Asterisks indicate where there is a significant difference between the steady state block of the indicated mutant channel and the WT (Student's *t* test: $*p < 0.05$, $**p < 0.01$, $^{\#}p = 0.057$).

The broken lines in B, D and F represent peak current inhibition in wild type (taken from Fig. 1 A). Channel block in C, E and G was estimated by subtracting "steady state" inhibition after 20 pulses in drug-free solution (Table 1) from channel block induced by 100μM or 300μM of qDil.

2.3.3 Modulation of channel gating by quaternary and tertiary diltiazem

To obtain insights into the link between state-dependent inhibition and channel gating we measured the standard characteristics of channel gating in control and the presence of drug. The activation and inactivation curves are shown in Fig. 4. Neither Dil (extracellular application) nor qDil (intracellular application) affected the activation curve of $Ca_V1.2$ (Fig. 4A, Table 2) and neither of them affected the kinetics of current activation and deactivation .

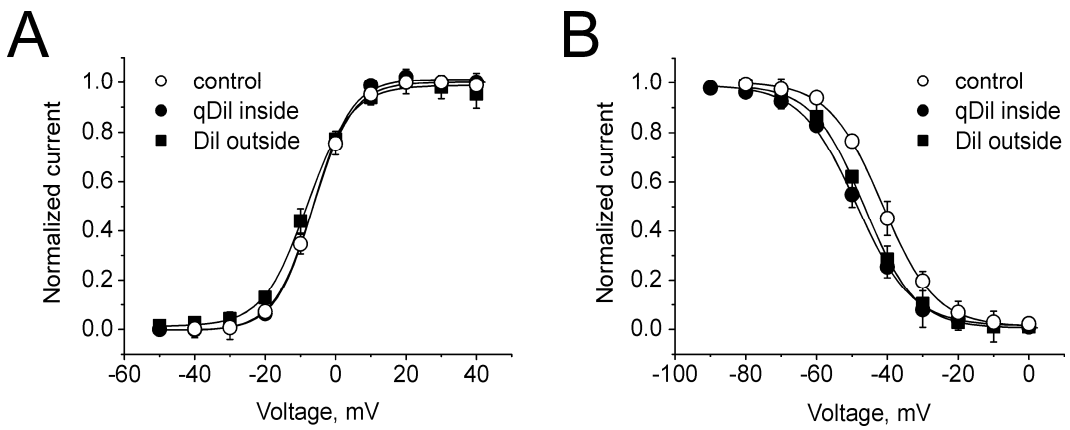

Fig. 4 Changes in channel gating induced by Dil and qDil.

Steady-state activation (A) and inactivation (B) of WT in the absence (open circles) or presence of 300 µM qDil applied from intracellular side (filled circles) or 300 µM of Dil applied by bath perfusion (filled squares, see Table 2 for parameters of the Bolzmann distributions).

Table 2 Effects of qDil and d-cis-diltiazem on voltage-dependent gating of $Ca_V1.2$

Midpoints and slope factors of the activation and inactivation curves and remaining current after 1000-ms pulse (r_{1000}) at 0 mV pulse (n=3÷6).

WT	$V_{0.5,act}$, mV	k_{act}, mV	$V_{0.5,inact}$, mV	k_{inact}, mV	r_{1000}, %
Control	-6.4±0.7	5.6±0.6	-41.4±1.0	7.4±0.9	69±6
300 µM qDil (intracellular)	-6.3±0.7	5.3±0.7	-48.5±0.9	7.7±0.8	44±11
300 µM Dil (extracellular)	-8.2±0.8	6.2±0.7	-46.4±1.2	7.2±1.1	38±10

In line with previous studies we observed a leftward shift of the inactivation curve by 300 µM Dil (5.0±1.5 mV). Quaternary diltiazem applied at the same concentration from the intracellular side induced a very similar shift (7.1±1.3 mV) suggesting similar state-dependency of both compounds (Fig. 4 B).

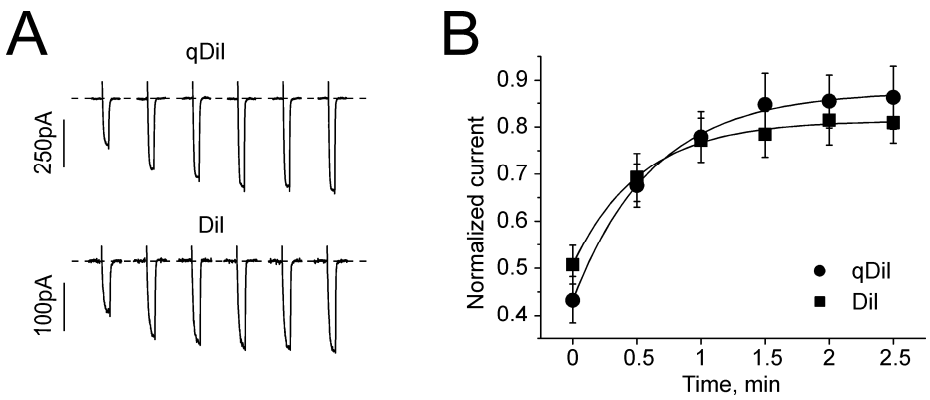

Fig. 5 Recovery of wild-type $Ca_V1.2$ from block by intracellularly applied qDil and extracellularly applied Dil.

A-B, Recovery from block by 300μM intracellular quaternary (circles) or 300μM extracellular tertiary diltiazem (squares) at -80mV holding potentials. Block was elicited by a standard conditioning train of 20 pulses in the presence of and recovery monitored by applying short (20 ms) test pulses at different time after the train. The mean time constants of recovery from block by Dil and qDil were 32.3±5.2 (n=7) and 37.1±4.9 (n=9) respectively.
Recovery from block by qDil and Dil was compared at a holding potential of -80 mV. Figure 5 illustrates the very similar recovery from block by intracellular qDil and extracellularly applied Dil (τ(qDil)=37.1±4.9 s vs. τ(Dil)=32.3±5.2 s).

2.4 DISCUSSION

$Ca_V1.2$ displays a high sensitivity to calcium antagonists such as DHPs, PAAs and diltiazem (Striessnig et al., 1991, Hockerman et al., 1997, Catterall et al., 2005). Calcium antagonists are clinically used to treat hypertension and angina pectoris (Fleckenstein et al., 1980, Triggle, 2007) PAAs and diltiazem are also used as antiarrhythmics and block L-type ($Ca_V1.2$) channels more efficiently at higher frequencies (Lee and Tsien, 1983).

Putative diltiazem binding determinants were identified on pore forming segments IIIS6 and IVS6 and the selectivity filter region (Hering et al., 1996; Kraus et al., 1998; Berjukov et al., 1999; Hockerman et al., 2000; Dilmac et al., 2003). A modulating role of channel inactivation in block by diltiazem was revealed in studies with mutant and chimeric $Ca_V1.2$ constructs (Berjukov et al., 1999; Dilmac et al., 2003; Motoike et al., 1999). Like PAAs,

diltiazem blocks $Ca_V1.2$ channels in a use-dependent manner (Hockerman et al., 2000; Lee and Tsien, 1983). The molecular mechanism of channel inhibition and the access path of diltiazem to its receptor site are, however, less understood. A quaternary BTZ (SQ32,428, Fig. 1D) was shown to block L-type channels in BC3H1 cells when applied from the extracellular side of the membrane in a non-use-dependent manner (Hering et al. 1993). Extracellular application of 100 and 300 µM of SQ32,428 on heterologously expressed $Ca_V1.2$ in the present study confirmed this observation. Tikhonov and Zhorov (2008) hypothesised that access of the "bulky BTZs" is unlikely to occur through the open activation gate from the intracellular side and proposed a "side walk" access of BTZ molecules from the extracellular side via the III/IV domain interface to their binding site in the pore. As shown in figure 1, qDil inhibited I_{Ba} predominantly when applied to the intracellular side of the membrane. The estimated tonic inhibition by intracellularly applied qDil was small (current density of -14.7 ± 0.9 pA/pF in control vs. –13.9 ± 1.1 pA/pF after first pulse in the presence of 300 µM qDil). Extracellular application (up to 300 µM) induced no use-dependent effect (Fig. 2 C) and only a low level of tonic current inhibition (Fig. 2 D). The more pronounced tonic I_{Ba} inhibition by Dil (Fig. 2 D) contributes to its concentration-inhibition relationship. This is evident from Fig. 1 B where stronger I_{Ba} inhibition by Dil was particularly evident at high drug concentrations (See Fig. 2 D).

Our principle finding that intracellularly applied qDil accesses its binding site through the open activation gate is in line with data of Smirnov and Aaronson (1998) who suggested that use-dependent current inhibition is induced by the charged form of diltiazem from inside. Furthermore, intracellular channel inhibition by qDil was modulated by four IIIS6 and three IVS6 mutations that have previously been identified as putative diltiazem binding determinants. Selectivity filter mutations less efficiently prevented channel block which is in line with Dilmac et al. 2003.

Taken together these data support a scenario where intracellularly applied qDil and extracellularly applied Dil interact with the same or largely overlapping binding pockets in the channel pore (Fig. 3).

Intracellular access of the permanently charged qDil to its binding site seems to occur in a very similar way as previously shown for quaternary PAAs. Quaternary PAAs approach their binding site on $Ca_V1.2$ from the intracellular face of the plasma membrane and repeated channel opening facilitates access of PAAs to the pore region which explains use-dependent block (Hescheler et al., 1982; Berjukov et al., 1996; Beyl et al. 2008). The access path of charged 1,4 DHPs occurs, however, via a pathway from the extracellular site of the membrane. Amlodipine in its ionised form and the permanently charged quaternary DHP derivative SDZ 207-180 were found to be ineffective when applied intracellularly, suggesting that the DHP receptor site is inaccessible from the intracellular surface while extracellular application of these compounds results in channel block indicating that these antagonists gain access to the receptor site via an extracellular pathway (Kass et al. 1991, see Hockerman et al. 1997 for review). It is tempting to speculate that DHPs reach their receptor determinants in the pore via the side walk access proposed by Thikhonov and Zhorov (2008).

2.4.1 Similar state dependency of Cav1.2 inhibition by qDil and Dil

High affinity binding to open and inactivated channel states are important characteristics of use-dependent channel blockers. In order to analyse drug accesses via the intracellular channel mouth we have co-expressed the α_1 subunit of Cav1.2 with the β_{2a} subunit which is known to prolong the open state by minimising channel inactivation. As shown in Figs 1 C, D the absence of inactivation during short pulses did not prevent use-dependent channel block suggesting access of qDil to its binding site via the open gate. Block development was slow and equilibrated at 300 µM over 15 100 ms pulses (Fig. 1 A). Slow block development is also evident from the acceleration of the current decay with 300 µM qDil in the pipette (Fig. 1 D) and the non significant changes in the steady state activation curve (Fig. 4 A) (see also Lee

and Tsien, 1983). However, channel inhibition is modulated by inactivation as evident from the shifts of the availability curves in Fig. 4 B (see also Zhang et al. 2010).

Accumulation of channel inhibition during a pulse train illustrated in Fig. 1 A depends on channel recovery between pulses. Recovery from use-dependent block by qDil and Dil was found to be very similar (Fig. 5, τ(qDil)=37.1±4.9 s vs. τ(Dil)=32.3±5.2 s). Similar recovery from block and similar apparent affinities (IC_{50}(Dil)= 95±5µM and IC_{50}(qDil) = 85±9µM) support the hypothesis that both compounds interact with identical or largely overlapping binding determinants in the channel pore.

The differences in tonic block observed for Dil and qDil warrants further research. The negligible "intracellular tonic I_{Ba} inhibition" induced by intracellular qDil (current density of -14.7 ± 0.9 pA/pF in control vs. –13.9 ± 1.1 pA/pF after first pulse in the presence of 300 µM qDil) suggests that the charged form induces predominantly use-dependent block, while the neutral form may be responsible for tonic inhibition (see also Smirnov and Aaronson, 1998). Access of the neutral form of Dil to its binding determinants in the pore via the side walk access (Thikhonov and Zhorov, 2008) can not be excluded.

2.5 Conclusions and outlook

Data of the present study demonstrate intracellular access of quaternary (membrane-impermeable) diltiazem and the interaction of qDil with determinants of the binding pocket previously identified for tertiary diltiazem (Hering et al., 1996; Hockerman et al., 2000; Dilmac et al., 2003). Quaternary diltiazem accesses its binding determinants via the inner channel mouth in a similar manner as was previously found with quaternary PAAs. Our data suggest that use-dependent block of $Ca_V1.2$ by diltiazem occurs predominantly via the open channel conformation.

Our study also permits new insights into the structure-activity relationship of this therapeutically important drug. A structurally related BTZ (SQ32,428) has no effect when

applied from the cytosolic side (Fig.2 A, C, see also Hering et al., 1993). Compared to SQ32,428 the C_5 of qDil is replaced by a sulfur atom and the trifluoromethyl group in position C_6 is substituted by a hydrogen atom. Additionally, the methyl group of SQ32, 428 in position C_3 is replaced by an acetoxy group (Fig. 2 B). Any of these apparently small structural differences may be essential for interaction of d-cis-diltiazem with its intracellular or extracellular accessible binding sites. Thikhonov and Zhorov, 2008 proposed an interesting concept how the functional groups of BTZ may interact with individual amino acid residues in the pore. Derivatives of quaternary diltiazem (with individually replaced moieties) may thus represent interesting tools for investigating the molecular basis of use-dependent drug interactions with intracellular accessible binding determinants.

2.6 REFERENCES

Berjukov S, Aczel S, Beyer B, Kimball SD, Dichtl, M, Hering S, et al. (1996). Extra- and intracellular action of quaternary devapamil on muscle L-type Ca(2+)-channels. *Br J Pharmacol* **119**: 1197-1202. Berjukov

Berjukow S, Gapp F, Aczel S, Sinnegger, M J, Mitterdorfer J, Glossmann H, et al. (1999). Sequence differences between alpha1C and alpha1S Ca2+ channel subunits reveal structural determinants of a guarded and modulated benzothiazepine receptor. *J Biol Chem* **274**: 6154-6160.

Catterall WA (2000). From ionic currents to molecular mechanisms: the structure and function of voltage-gated sodium channels. *Neuron* **26**: 13-25.

Catterall WA, Perez-Reyes E, Snutch TP, Striessnig J (2005). International Union of Pharmacology. XLVIII. Nomenclature and structure-function relationships of voltage-gated calcium channels. *Pharmacol Rev* **57**: 411-425.

Dilmac N, Hillard N, Hockerman GH (2003). Molecular determinants of Ca2+ potentiation of diltiazem block and Ca2+-dependent inactivation in the pore region of cav1.2. *Mol Pharmacol* **64**: 491-501.

Ellis SB, Williams ME, Ways NR, Brenner R, Sharp AH, Leung AT, et al. (1988). Sequence and expression of mRNAs encoding the alpha 1 and alpha 2 subunits of a DHP-sensitive calcium channel. *Science* **241**: 1661-1664.

Fleckenstein A, Fleckenstein-Grun G (1980). Cardiovascular protection by Ca antagonists. *Eur Heart J* **1**(Suppl B): 15-21.

Hamill OP, A. Marty A, Neher E, Sakmann B, Sigworth FJ (1981). Improved patch-clamp techniques for high-resolution current recording from cells and cell-free membrane patches. *Pflugers Arch* **391**: 85-100.

Hering S, Savchenko A, Strubing C, Lakitsch M, Striessnig J. (1993). Extracellular localization of the benzothiazepine binding domain of L-type Ca2+ channels. *Mol Pharmacol* **43**: 820-826.

Hering S, Aczel S, Grabner M, Doring F, Berjukow S, Mitterdorfer J, et al. (1996). Transfer of high sensitivity for benzothiazepines from L-type to class A (BI) calcium channels. *J Biol Chem* **271**: 24471-24475.

Hescheler J, Pelzer D, Trube G, Trautwein W (1982). Does the organic calcium channel blocker D600 act from inside or outside on the cardiac cell membrane? *Pflugers Arch* **393**: 287-291.

Hille B (1984) Ionic Channels of Excitable Membranes. *Sinauer Associates, Sunderland, MA, USA*; 1st Edition.

Hockerman GH, Peterson BZ, Johnson BD, Catterall WA (1997). Molecular determinants of drug binding and action on L-type calcium channels. *Annu Rev Pharmacol Toxicol* **37**: 361-396.

Hockerman GH, Dilmac N, Scheuer T, Catterall WA (2000). Molecular determinants of diltiazem block in domains IIIS6 and IVS6 of L-type Ca(2+) channels. *Mol Pharmacol* **58**: 1264-1270.

Kass R, Arena JP, Chin S (1991). Block of L-type calcium channels by charged dihydropyridines: sensitivity to side of application and calcium. *J. Gen. Physiol.* **98**:63–75.

Kraus RL, Hering S, Grabner M, Ostler D, Striessnig J (1998). Molecular mechanism of diltiazem interaction with L-type Ca2+ channels. *J Biol Chem* **273**: 27205-27212.

Lee KS, Tsien RW (1983). Mechanism of calcium channel blockade by verapamil, D600, diltiazem and nitrendipine in single dialysed heart cells. *Nature* **302**: 790-794.

Mathias RT, Cohen IS, Oliva C (1990). Limitations of the whole cell patch clamp technique in the control of intracellular concentrations. *Biophys J* **58**: 759-770.

Motoike HK, Bodi I, Nakayama H, Schwartz A, Varadi G. (1999). A region in IVS5 of the human cardiac L-type calcium channel is required for the use-dependent block by phenylalkylamines and benzothiazepines. *J Biol Chem* **274**: 9409-9420.

Schulla V, Renström E, Feil R, Feil S, Franklin I, Gjinovci A, et al (2003). Impaired insulin secretion and glucose tolerance in beta cell-selective Ca(v)1.2 Ca2+ channel null mice. *EMBO J* **22**: 3844-3854.

Sinnegger-Brauns MJ, Hetzenauer A, Huber IG, Renström E, Wietzorrek G, Berjukov S, et al (2004). Isoform-specific regulation of mood behavior and pancreatic beta cell and cardiovascular function by L-type Ca 2+ channels. *J Clin Invest* **113**: 1430-1439.

Smirnov SV, Aaronson PI (1998). pH-dependent block of the L-type Ca2+ channel current by diltiazem in human mesenteric arterial myocytes. *Eur J Pharmacol* **360**: 81-90.

Striessnig J, Murphy BJ, Catterall WA (1991). Dihydropyridine receptor of L-type Ca2+ channels: identification of binding domains for [3H](+)-PN200-110 and [3H]azidopine within the alpha 1 subunit. *Proc Natl Acad Sci U S A* **88**: 10769-10773.

Striessnig J, Grabner M, Mitterdorfer J, Hering, S, Sinnegger MJ, Glossmann H (1998). Structural basis of drug binding to L Ca2+ channels. *Trends Pharmacol Sci* **19**: 108-115.

Striessnig J (1999). Pharmacology, structure and function of cardiac L-type Ca(2+) channels. *Cell Physiol Biochem* **9**: 242-269.

Tikhonov DB, Zhorov BS (2008). Molecular modeling of benzothiazepine binding in the L-type calcium channel. *J Biol Chem* **283**: 17594-17604.

Triggle DJ (2007). Calcium channel antagonists: clinical uses—past, present and future. *Biochem Pharmacol* **74**: 1-9.

Uehara A , Hume JR (1985). Interactions of organic calcium channel antagonists with calcium channels in single frog atrial cells. *J Gen Physiol* **85**: 621-647.

Zhang HY, Liao P, Wang JJ, Yu de J, Soong TW (2010). Alternative splicing modulates diltiazem sensitivity of cardiac and vascular smooth muscle Ca(v)1.2 calcium channels. *Br J Pharmacol*. **160**:1631-1640.

3 CHAPTER III

T1143 ESSENTIAL FOR $CA_V1.2$ INHIBITION BY DILTIAZEM:

REFINED DRUG BINDING MODEL

MS by Shabbier et al. in preparation

3.1 INTRODUCTION

Calcium channel inhibitors are widely used as cardiovascular therapeutics and serve as important tools to probe the structure and function of this ion channel family (Beyl et al. 2007). L-type calcium channels are inhibited by 1,4-dihydropyridines (DHPs), phenylalkylamines (PAAs) and benzothiazepines (BTZ). Diltiazem (Dil) chemically belongs to the BTZ and is used to treat hypertension, angina pectoris, arrhythmias and other cardiovascular disease (Triggle 2003, 2006, 2007; Zhang et al. 2003). Like PAAs Dil inhibits L-type channels in a state-dependent manner (Lee and Tsien 1983). Resting state block is evident from current inhibition in the absence of channel activation or at low pulse frequency (Berjukow et al. 1999). High-affinity interaction of Dil with open and inactivated channels is shown by channel block developing during repetitive pulsing ("use-dependence") and from a drug-induced shift of the steady-state inactivation curve (Lee and Tsien 1983), (Uehara and Hume 1985). Also, L-type channels are more efficiently inhibited by Dil when Ca^{2+} rather than Ba^{2+} is used as a charge carrier (Lee and Tsien 1983).

Experiments with the photoreactive diltiazem-like antagonist [3H]benziazem indicated that key binding determinants of Dil on L-type Ca^{2+} channels are located on transmembrane segments IIIS6 and IVS6 of the pore-forming α1C-subunit (Kraus et al. 1996). This was later confirmed in systematic mutation studies where six residues in segment IIIS6 (I1150, I1153, I1156, M1160, F1164 and V1165) and three residues in segment IVS6 (I1460, Y1463 and M1464) were identified as determinants of Dil sensitivity (Dilmac et al. 2003; Hering et al. 1996; Hockerman et al. 2000; Hockerman et al. 1997; Hockerman et al. 1995; Kraus et al. 1998). Dilmac et al. (2003) concluded that three (Hockerman et al. 1995) residues in the selectivity filter region (E1118, E1419, and F1117) modulate channel inhibition with Ca^{2+} as charge carrier (Dilmac et al. 2003). Removal of inactivation by point mutations in S6 segments can diminish channel block by Dil (Berjukow et al. 1999; Hering et al. 1997; Kraus et al. 1998; Motoike et al. 1999). This "allosteric modulation" complicates the identification of the putative drug binding site (Hering 2002). The access path of BTZ to their binding site in Cav1.2 is still controversial (see (Tikhonov and Zhorov 2008). We have, however, recently shown that the

quaternary (membrane-impermeable) diltiazem (qDil) accesses its binding pocket via an intracellular pathway in a use-dependent manner (Shabbir et al.)

Several homology models were recently developed for the open pore of Cav1.2, where key determinants of calcium channel blockers are located (Bruhova et al. 2008; Bruhova and Zhorov; Stary et al. 2008; Tikhonov and Zhorov 2008).

By docking a BTZ (SQ32910) into a homology model of transmembrane segments S5, S6 and P-loops of the four domains of α1C, Tikhonov and Zhorov (2008) proposed the first three-dimensional model of the BTZ binding site. The Tikhonov-Zhorov model integrates the results of previous mutational studies and enabled insights into the putative binding pocket for Dil.

Structure-activity relationships of BTZs reveal that (Das et al. 1992; Floyd et al. 1992; Kimball et al. 1992) the blocking potency is affected by the configurations of the chiral centers and modification of the substituents of the BTZ rings.

In line with mutational studies, the Tikhonov-Zhorov model integrates Y1463 as possible H-bonding site. Other potential H-bond interactions in vicinity of the BTZ binding pocket were discussed, but not included in the model (Tikhonov and Zhorov 2008).

COMFA models suggest, however, that BTZ interact with their receptor through a negative charge site, two hydrogen-bonding sites, and three hydrophobic regions (Corelli et al. 1997) et al, 1997).

In the present study, we first analyzed potential H-bond interactions of Dil in a homology model of the open Cav1.2 pore structure. This process led to identification of residues T1067, S1142 and T1143 as candidates for H-bond contacts. These residues were then individually mutated to alanine in order to study the effects on channel inhibition by Dil. In our study we made use of Dil and its quaternary derivative interacting with the intracellular accessible binding site (Shabbir et al.). T1143 was identified as a novel strong determinant of Dil sensitivity. We propose a refined model of the Dil binding site on $Ca_V1.2$.

3.2 EXPERIMENTAL PROCEDURES

Mutagenesis- The $Ca_V1.2$ α_1-subunit coding sequence (GenBank™X15539) in-frame 3' to the coding region of a modified green fluorescent protein (GFP) was kindly donated by Dr. M. Grabner (Grabner

et al. 1998). Substitutions in segment IIIS5, IIISF of the $Ca_V1.2$ α_1-subunit were introduced using the QuikChange® Lightning Site-Directed Mutagenesis Kit (Stratagene) with mutagenic primers according to the manufacturer's instructions. Mutations were introduced in segment IIIS5 in position T1067A and in the selectivity filter of domain III in positions S1142A and T1143A. All constructs were checked by restriction site mapping and sequencing.

Cell culture and transient transfection- Human embryonic kidney tsA-201 cells were grown at 5% CO2 and 37°C to 80% confluence in Dulbecco's modified Eagle's/F-12 medium supplemented with 10% (v/v) foetal-calf serum and 100 units/ml penicillin/streptomycin. Cells were split using trypsin/EDTA and plated on 35-mm Petri dishes (Falcon) at 30–50% confluence 16 h before transfection. Subsequently tsA-201 cells were co-transfected with cDNAs encoding wild-type (GenBankTM accession number X15539) or mutant CaV1.2 α1-subunits (T1067A, S1142A, T1143A), with auxiliary β2a- and α2δ-subunits (Ellis et al. 1988). The transfection of tsA-201 cells was performed using the FuGENE 6 transfection reagent (Roche Applied Science) following standard protocols.

Ionic current recordings and data acquisition— Barium currents (I_{Ba}) through voltage-gated Ca^{2+} channels were recorded at 22–25°C using the whole-cell patch clamp configuration (Hamill et al. 1981) by Axopatch 200A patch clamp amplifier (Axon Instruments) 36–48 h after transfection. The extracellular bath solution contained 20 mM $BaCl_2$, 1 mM $MgCl_2$, 10 mM HEPES, and 140 mM choline-Cl, titrated to pH 7.4 with methanesulfonic acid. The borosilicate glass patch pipettes (Harvard Apparatus, Holliston, MA, USA) with resistances of 1–4 MΩ were pulled and polished using a DMZ universal puller (Zeitz Instruments, Martinsried, Germany), and were filled with pipette solution containing 145 mM CsCl, 3mM $MgCl_2$, 10 mM HEPES, and 10 mM EGTA, titrated to pH 7.25 with CsOH. Quaternary diltiazem was dissolved for intracellular application in the internal (pipette) solution and for extracellular application in bath saline. Intracellular application was done via the patch pipettes and I_{Ba} were recorded 5 min after the whole cell configuration was established. To assure that that the internal drug concentration reached steady state, use-dependent block was monitored after different time intervals. An approximation of the time for intracellular perfusion (Mathias et al. 1990) predicts that under our experimental conditions, an equilibrium between the pipette concentration of (+)qDiltiazem and the intracellular solution should be reached within about

10s. For extracellular application, the drug was applied to cells under voltage clamp using a microminifold perfusion system (ALA scientific Instruments Westbury, NY) and I_{Ba} were recorded after a 5-min equilibration period. Use-dependent Ca^{2+} channel block was estimated as peak I_{Ba} inhibition during short (100 ms) test pulses from –80 mV at a frequency of 0.2 Hz. The dose-response curves of *I*Ba inhibition were fitted using the Hill equation, *I*Ba, drug/*I*Ba, control (in %) = (100 – *A*)/(1+(*C*/IC50)*n*H) + *B*, where IC50 is the concentration at which *I*Ba inhibition is half-maximal, *A* is the applied drug concentration. *I*Ba-unblock from use-dependent inhibition by qDiltiazem was studied by applying a 20-ms test pulse at various time intervals after the last pulse of the train.

All data were digitized using a DIGIDATA 1200 interface (Axon Instruments), smoothed by means of a four-pole Bessel filter, and stored on computer hard disc. Leak currents were subtracted digitally using average values of scaled leakage currents elicited by a 10-mV hyperpolarizing pulse. Series resistance and offset voltage were routinely compensated for. The pClamp software package (version 7.0 Axon Instruments, Inc.) was used for data acquisition and preliminary analysis. Microcal Origin 7.0 was used for analysis and curve fitting.

Molecular modelling- The structure of the open Cav1.2 pore model was taken from Stary et al., 2008. Refinement of the binding pocket, the P-helix and the selectivity filter region of domain III are described in detail in the results section.

The structure of Dil was downloaded from the pubchem database and geometry optimized with the Hartee-Fock 3-21G basis set implemented in Gaussian03 (Frisch et al, 2003).

Initially the drug was placed manually into the BTZ binding site, and the OPLS 2001 force field was used to energy-minimize the complex. Subsequent docking was performed with the program Gold 4.0.1 using the Gold scoring function. Side-chains of residues M1160, F1164 and Y1463 were taken from rotameric libraries (Cite GOLD). 150,000 operations of the GOLD genetic algorithm were used to dock diltiazem into the Cav1.2 model. The best-ranked 10 poses of each docking run were used for visual analysis of binding.

3.3 RESULTS

3.3.1 Model predictions of potential H-bond interactions with Dil.

In order to identify amino acids capable of forming H-bonds with Dil we made use of our previously published homology model of the Cav1.2 pore in open conformation (Stary et al. 2008). Visual inspection of the 3D coordinates suggested three polar candidate residues for H-bond formation (T1067 in IIIS5, S1142, and T1143 in the IIISF) in close proximity (~ 6 Å) to known binding residues (Fig. 1).

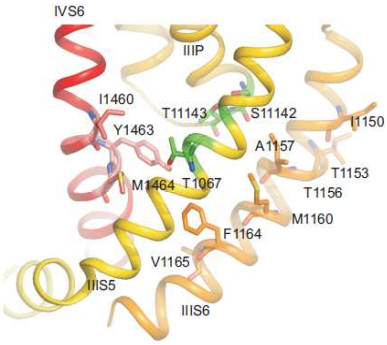

Fig 1.Diltiazem binding site in Cav1.2 homology model

Known binding residues in domains III and IVS6 are shown as orange or red sticks. A cluster of putative candidate residues for H-bond formation from helix IIIS5 and the selectivity filter of domain III are shown as green sticks.

These amino acids were subsequently mutated to alanine and their contributions to channel inhibition by Dil or qDil analysed in functional studies.

3.3.2 Use-dependent block of T1143A.

Barium (Ba^{2+}) currents through Cav1.2 were measured with the patch clamp technique in tsA-201 cells expressing α1C and the auxiliary β_{2a} and α_2-δ_1-subunits. Using the quaternary derivative (qDil) we have recently shown that Dil accesses its binding site from the intracellular side (Shabbier et al., 2010). To exclude complications by potential extracellular effects, we applied qDil via the patch pipette and analyzed current inhibition in candidate mutants T1067A (IIIS5), S1142A, T1143A (IIISF). I_{Ba} inhibition was first induced with 100 and 300µM qDil applied to the pipette using pulse

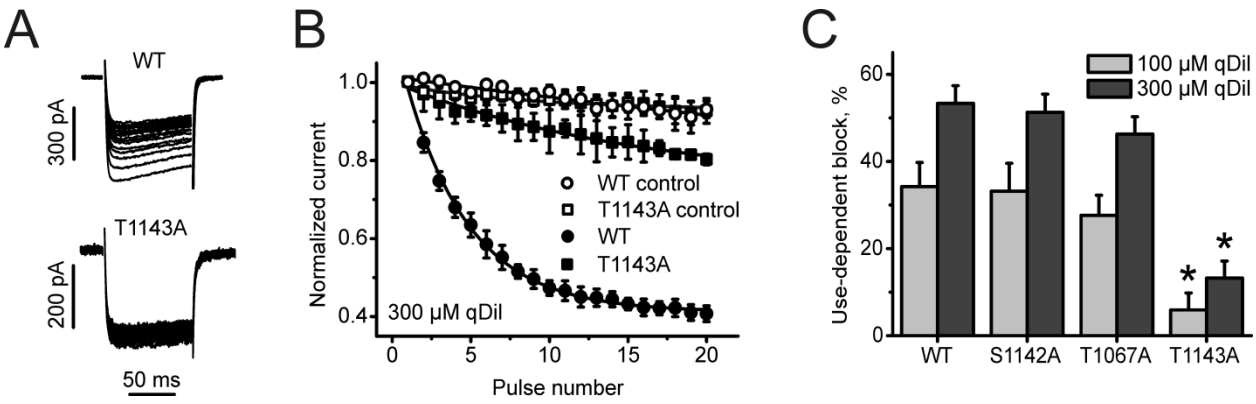

Fig 2.**Use-dependent block of $Ca_V1.2$ by intracellularly applied quaternary diltiazem**.

A, representative traces of I_{Ba}current through WT Cav1.2 and T1143A channels in the presence of 300µM qDil. B, use-dependent inhibition of wild-type and mutant channels was measured in the absence or presence of 100µM and 300µM qDil in the pipette (intracellular) solution. Channel block was estimated as peak I_{Ba} inhibition during trains of 20 pulses (0.2 Hz, 100 ms) applied from a holding potential of -80 mV to +20 mV. C**,** Use-dependent block accumulated after 20 pulses in WT and indicated mutants. Channel block was estimated as the difference between normalized current in presence of 100/300µM qDil and in absence of drug. Asterisks denote that the block value for quaternary diltiazem of the indicated mutant channel is significantly different from that of WT (Student's *t* test: **P*< 0.05)

trains applied at a frequency of 0.2 Hz. As shown in Fig. 2C, only T1143A significantly reduced sensitivity to qDil (Fig. 2 B) compared to wild type.

Similar findings were made with tertiary diltiazem (Dil). As shown in Figs. 4 and 8, T1143A prevented use-dependent I_{Ba} inhibition. Mutating the other candidate residues to alanine (T1067A and S1142A) did not change channel inhibition by 300 µM qDil (Fig. 2C).

3.3.3 Use-dependent block of other T1143 mutants.

Next we replaced T1143 with different residues to determine how the physicochemical properties of the amino acid side chain affected channel block. All mutants displayed reduced current inhibition

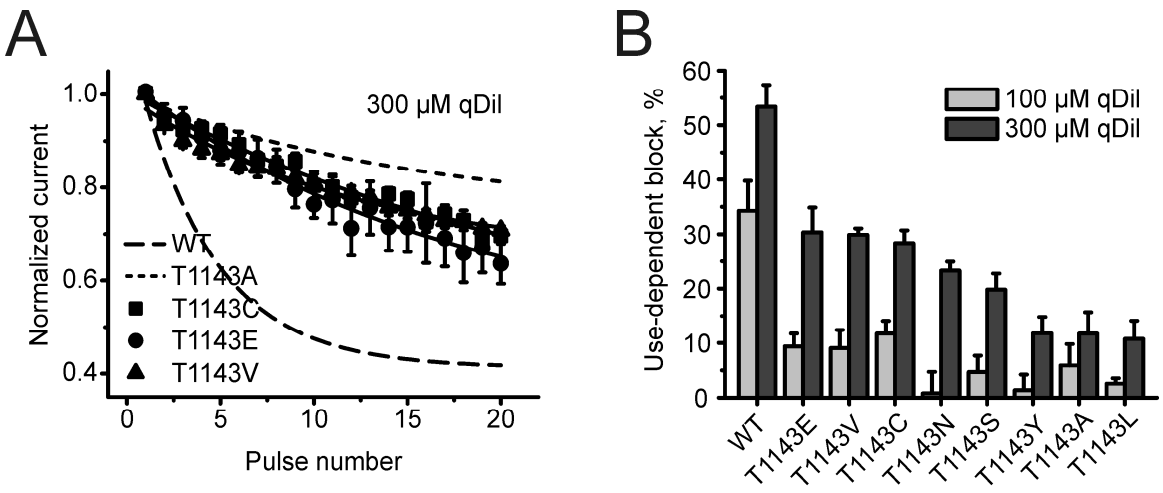

Fig 3. **Effect of other T1143 mutations on Cav1.2 inhibition by qDil**

A, use-dependent inhibition of T1143 mutant was measured in the absence or presence of 300 μM qDil in the pipette solution. Channel block was estimated as peak I_{Ba} inhibition during trains of 20 pulses (0.2 Hz, 100 ms) applied from a holding potential of –80 mV to +20 mV. B**,** Use-dependent block accumulated after 20 pulses in WT and indicated mutants. Channel block was estimated as the difference between normalized current in presence of 100/300μM qDil and in absence of drug.

Table 1. Peak current decay in the presence of qDil after 20 pulses (100 ms) at 0.2 Hz

Mutation	Use-dependent block, %	
	100 μMqDil	300 μMqDil
WT	34.2 ± 5.5	53.3 ± 4.0
T1143E	9.3 ± 2.3	30.3 ± 4.5
T1143V	9.0 ± 3.3	29.8 ± 1.1
T1143C	11.7 ± 2.3	28.3 ± 2.3
T1143N	0.7 ± 3.9	23.2 ± 1.6
T1143S	4.7 ± 2.9	19.7 ± 2.9
T1143Y	1.3 ± 2.8	11.7 ± 3.0
T1143A	5.8 ± 3.9	11.7 ± 3.9
T1143L	2.5 ± 1.01	10.7 ± 3.3

compared to wild type. However, as shown in Fig. 3 B, mutants T1143E/V/C/N/S were more efficiently blocked than constructs T1143A/Y/L. (See table 1 for block by values of, 100 and 300µM qDil block). As shown in Figs. 4 and 8, T1143A prevented use-dependent I_{Ba} inhibition of Diltiazem. Mutating the other candidate residues to alanine (T1067A and S1142A) did not change channel inhibition by 300 µM qDil (Fig. 2C).

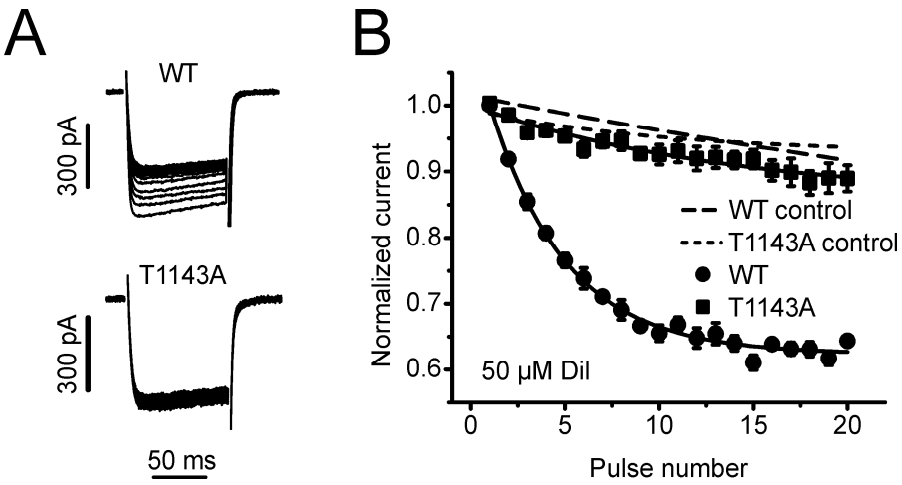

Fig 4. **T1143A abolishes block by Diltiazem**

A, representative traces of I_{Ba}current through WT and T1143A channels in the presence of extracellularly applied 50 µM Dil. B, use-dependent inhibition of wild-type and T1143A channelswas measured in the absence or presence of 50 µM Diltiazem in the bath. Channel block was estimated as peak I_{Ba} inhibition during trains of 20 pulses (0.2 Hz, 100 ms) applied from a holding potential of –80 mV to +20 mV.

3.3.4 Mutation T1143A does not affect channel gating.

Changes in channel gating may have allosteric effects on Cav1.2 inhibition by calcium antagonists (Hering, 2002). We therefore investigated possible changes in channel gating by measuring the activation and inactivation curves with the mutant T1143A. T1143A does not shift the activation (ΔV_{act} = –5.7±0.7 mV) and inactivation curve (–43.7±0.7) compared to WT (ΔV_{act} = –6.5±0.7 and inactivation –42.8±0.8mV. A family of inward Ba^{2+} currents and the corresponding current-voltage (I-V) curve of mutant T1143A are shown in Fig. 5 and Table 3.

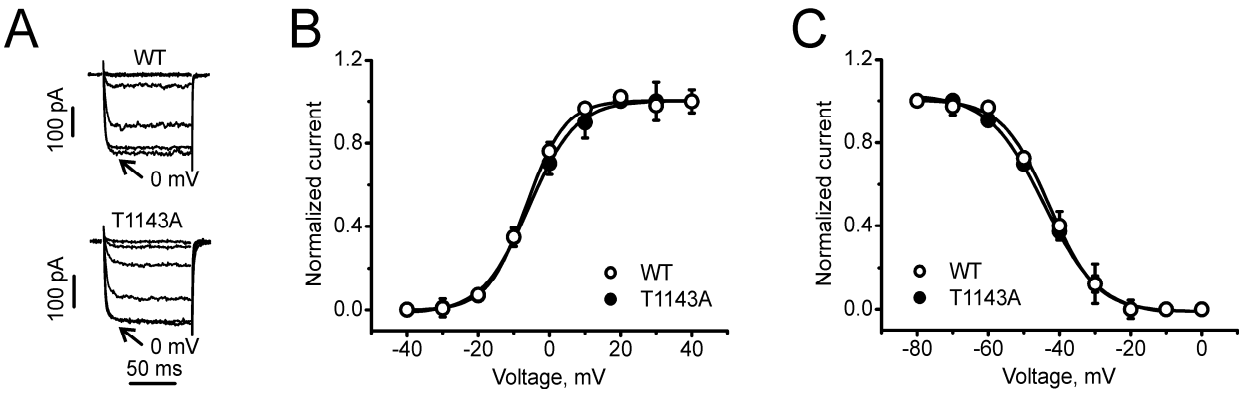

Fig 5. Kinetics of I_{Ba} through wild-type $Ca_v1.2$ and T1143A.

A, representative traces of I_{Ba}current through WT and T1143A channels.

B, normalized current-voltage relationships of the wild-type (n = 9, open circles) and T1143A (n = 11) channels. Potentials of half-maximal activation (V0.5,act) are –6.5 ± 0.7 mV and -5.7 ± 0.7 mV, for wild-type, and T1143A mutant channels, respectively. C, average voltage dependencies of steady-state inactivation for wild-type (n = 4, open circles) and T1143A (n = 4, filled squares) mutant channels. Solid lines represent fits to Boltzmann functions. Potentials of half-maximal inactivation (V0.5, inact) are –42.8, -± 0.8 mV, -43.7 ± 0.7 mV, for wild-type and T1143A and mutant channels respectively.

3.3.5 Frequency dependence of block.

To determine whether T1143A is accessible for qDil at high frequency, we tested Cav1.2 inhibition during 1 Hz pulse trains. Fig. 6 illustrates the corresponding use-dependent block. The strong reduction of IBa inhibition by T1143A was confirmed with 50µM of tertiary Dil that was applied by bath perfusion (Figs. 4 and 8).

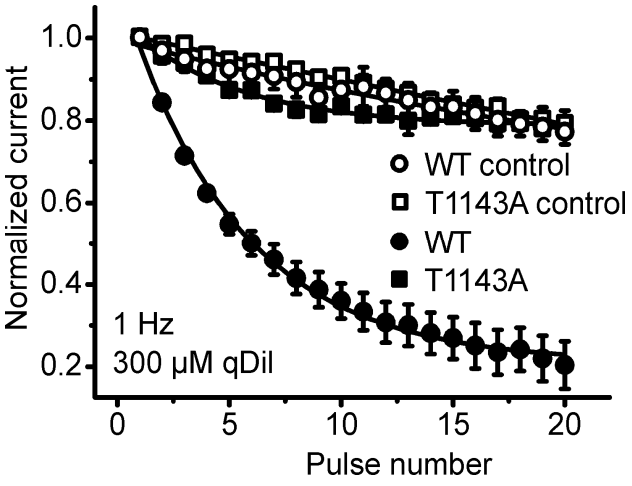

Fig 6. T1143A diminishes qDIl block at 1Hz frequency

Use-dependent inhibition of wild-type and T1143A mutant channels was measured in the absence (open symbols) or presence of 300 µm qDil (closed symbols) in the pipette (intracellular) solution.

3.3.6 Putative Diltiazem binding mode—comparison with SAR studies and COMFA model.

Docking was used to investigate putative interactions of T1143 with diltiazem. Initially, the drug was placed manually into the cavity followed by stepwise energy minimizations with the OPLS forcefield. Guided by the size of the drug molecule, the P-helix and the selectivity filter region of domain III were slightly adjusted to accommodate Dil. This drug-guided model refinement resulted in an upward shift of the IIIP domain of approximately 1.5 Å. These structural changes increased the numbers of favorable hydrogen bonds in domain III. New

hydrogen bonds are formed between Q1070 (IIIS5) and S1142 and T1143 (IIISF). The hydroxyl group of Y1152 (IIIS6) binds to the hydroxyl group of S1142 (IIISF) and the backbone carbonyl oxygen of V1141 (C-terminus of III-P helix). The hydroxyl group of Y1463 (IVS6) binds to the hydroxyl group of T1066 (IIIS5) and backbone oxygen atom of T1067 (see supplementary Fig. 2). The stability of this drug-refined model was tested in a 40-ns MD simulation (see supplementary information). This model was subsequently used to perform docking simulations. The program GOLD was employed to generate binding poses of diltiazem in the open Cav1.2 cavity utilizing its scoring function. Fig. 7A shows the binding mode of diltiazem that is in best agreement with experimental data. Hydrogen bonds are predicted between diltiazem and the hydroxyl group of T1143 from the selectivity filter of domain III. The polycyclic core of the drug is tightly packed with hydrophobic residues M1160 and F1164. Additional hydrophobic interactions are predicted with residues I1156 and A1157. The location of the negative charge, which does not directly interact with the glutamates from the EEEE locus, is marked with an asterisk. The positively charged nitrogen is oriented toward the base of the selectivity filter. Our model suggests that M1464 does not directly interact with diltiazem, as this residue is located within 6 Å of the drug. M1464 could, however, provide weak hydrophobic interactions (depending on the docking pose). Fig. 7B illustrates the agreement between the features suggested by the docking pose and the QSAR study by Corelli et al, 1997. Hydrophobic residues I1150 and I1153 are not within 6 Å of the drug. This observation agrees with the Tikhonov-Zhorov model, where allosteric effects for some BTZ sensitive residues, not directly interacting with drugs in their model, have been proposed.

To further analyse this, all 100 docking poses in the open conformation were considered. However, in none of them did all ten experimentally determined binding determinants directly interact with diltiazem at the same time.

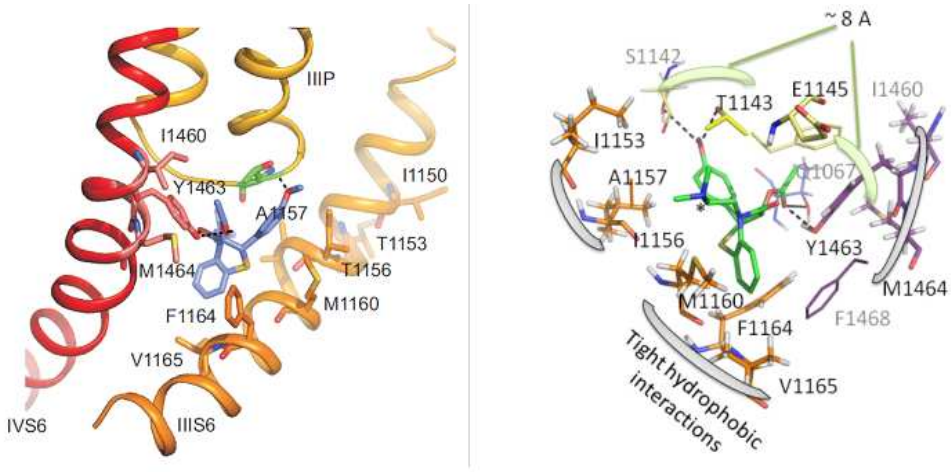

Fig 7. Putative Binding mode of diltiazem in the open Cav1.2 channel

A, Known binding residues are shown as orange (IIIS6) and red (IVS6) sticks. The newly identified binding determinant T1143, located at the base of the selectivity filter in domain III is shown in green. Black dots represent hydrogen bonds between diltiazem (blue sticks) and T1143 and Y1463.

B, Agreement between the QSAR features (Corelli et al, 1997) and the best docking pose. Hydrophobic interactions are marked grey; polar interacting regions are shaded green. The distance between the two hydrogen bonding features is approximately 8 Å. The location of the positive charge is marked with an asterix.

3.4 DISCUSSION

3.4.1 Threonine 1143 is a strong determinant of Dil sensitivity.

We have previously shown that qDil accesses its binding site in the open channel pore from the intracellular site in a use-dependent manner (Shabbir et al 2010). Here we made use of Dil and qDil to identify additional binding determinants for this clinically important drug. Structure-activity relationship studies of BTZ suggest the importance of 2 H-bonds for high affinity block (e.g. (Das et al. 1992; Floyd et al. 1992; Kimball et al. 1992), Consequently we focused on polar residues surrounding an *in silico* binding pocket that was designed based on

previous work of (Tikhonov and Zhorov 2008). Out of the three identified candidate residues, mutation T1143A almost completely eliminated channel inhibition by qDil and Dil, while the other mutations (T1067A, S1142A) had no effect (Fig. 2C). At 300 µM Dil, T1143A completely stopped use-dependent channel block at 1 Hz (Fig. 6). The concentration-inhibition relationship for Cav1.2 incorporating the β2a-subunit at low frequency (0.05 Hz) is illustrated in Fig. 8. Channel block at the highest concentration applied (500 µM) was 70±5.0 %. To our knowledge this is the strongest effect on Dil sensitivity reported for a single amino acid mutation (Hockerman et al. 2000).

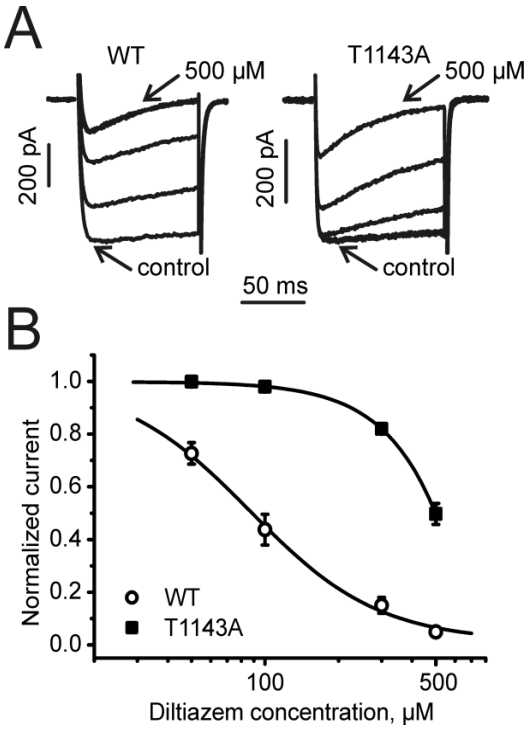

Fig 8. Diltiazem block of WT and T1143A

The IC50 values control to 500µM [d-*cis*-diltiazem: 95 ± 5 mM (data from shabbir et al 2010) (Hill slope *n*H = 1.6 _ 0.4) WT and T1143A were obtained by fitting the data points to the Hill equation (as described in Methods). Channel block was estimated as peak I_{Ba} inhibition during trains of 20 pulses (0.2 Hz, 100 ms) applied from a holding potential of -80 mV to +20 mV in control (Table 2).

Table 2. Peak current decay in the absence of drug after 20 pulses (100 ms) at 0.2 Hz

Mutation	Control inhibition, %
WT	5.9 ± 3.4
T1143E	6.3 ± 1.3
T1143V	6.1 ± 0.2
T1143C	2.2 ± 1.6
T1143N	13.1 ± 0.1
T1143S	9.4 ± 0.6
T1143Y	35.1 ± 0.1
T1143A	7.5 ± 3.1
T1143L	16.1 ± 0.3
S1142A	6.2 ± 3.3
T1067A	5.5 ± 3.1

T1143 was suggested to interact with the BTZ SQ32910 by (Tikhonov and Zhorov 2008) using an *in silico* docking approach. In our homology model, T1143 lies in close proximity with previously identified binding modulating residues E1118 and F1117 from the selectivity filter (Fig. 1). Interestingly, it was previously reported that T1143A reduces I_{Ba} inhibition by verapamil during a 1-Hz train by approximately 25% (Dilmac et al. 2004). We have confirmed this finding making use of quaternary devapamil (100 µM) applied via the pipette (Fig. 9).

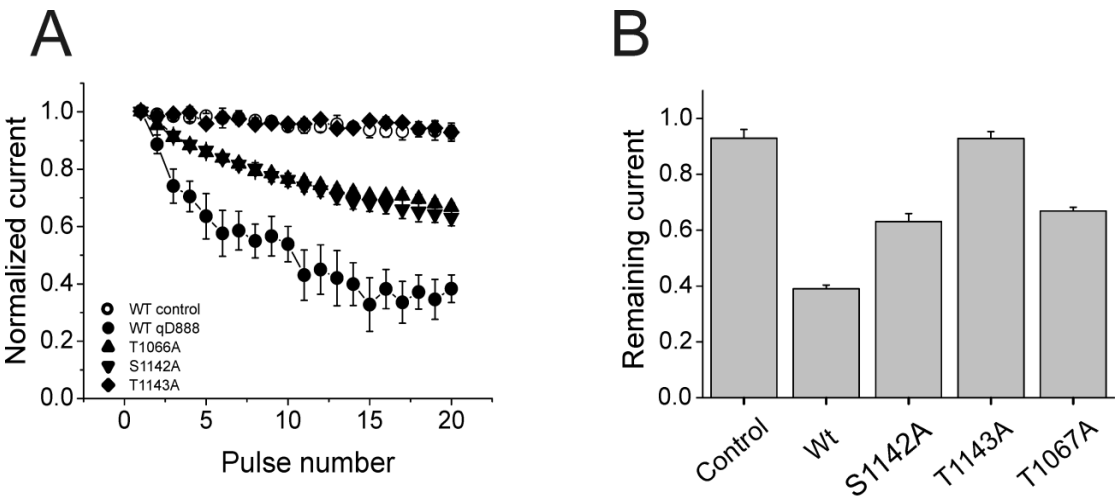

Fig 9. T1143A diminish the Use dependent block of qD888

A,use-dependent inhibition of wild-type and mutant channels was measured in the absence or presence of 100 μM qD888 in the pipette (intracellular) solution. Channel block was estimated as peak I_{Ba} inhibition during trains of 20 pulses (0.2 Hz, 100 ms) applied from a holding potential of -80 mV to +20 mVB**,** Remaining currents after 20 pulses in WT and the indicated mutants.

Taken together, these findings indicate that T1143 forms part of the PAA and Dil binding sites. However, substitution of this residue by alanine has a much stronger effect on channel block by Dil than by by PAAs. This data suggests that T1143 is essential for binding of Dil and less important for channel inhibition by PAAs. Comparison of the binding modes proposed by docking simulations provides a rationale for the different effects of T1143. While T1143 and Y1463 seem to be important anchors for Dil, phenyalalkylamines such as verapamil or quaternary devapamil are apparently anchored in the cavity by formation of hydrogen bonds with Y1463 and Y1152 (IIIS6) Fig 10.

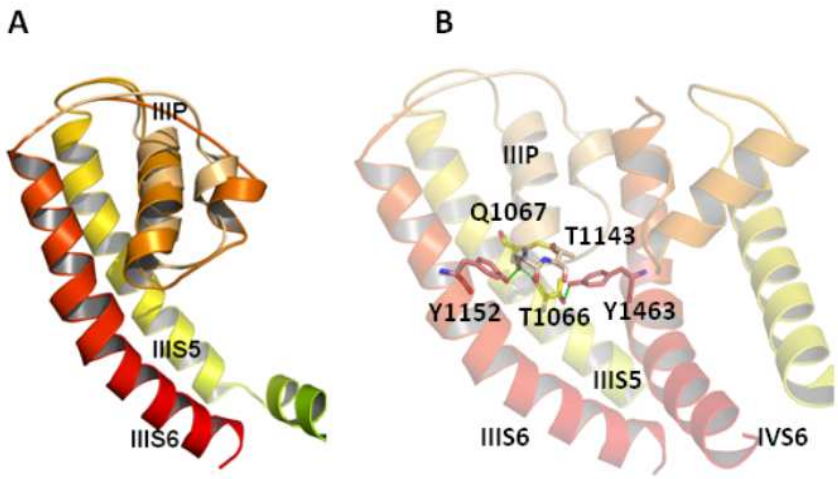

Fig 10. Hydrogen bonding of Tyrosines with IIIS6 and IVS6

A, Superposition of original IIIP loop (dark orange) and slightly shifted IIIP loop (light orange).

B, the modifications lead to improved hydrogen bonding networks (green) between segments III-S5, III-P, III-S6, and IV-S6. New hydrogen bonds are formed between Q1070 (IIIS5) and S1142 and T1143 (IIISF). The hydroxyl group of Y1152 (IIIS6) binds to the hydroxyl group of S1142 (IIISF) and the backbone carbonyl oxygen of V1141 (C-terminus of III-P helix). The hydroxyl group of Y1463 (IVS6) binds to the hydroxyl group of T1066 (IIIS5) and backbone oxygen atom of T1067.

3.4.2 T1143A displays wild type kinetics.

Changes in channel gating have been shown to affect channel inhibition by calcium antagonists (Berjukow et al. 2000; Sokolov et al. 2001). We therefore carefully studied the kinetics of mutant T1143A. Fig. 5 illustrates that introduction of an alanine in position T1143 affected neither the channel's activation nor its inactivation properties. Both curves were indistinguishable from wild type (see also Table 3). This finding supports the view that reduced channel block caused by T1143A reflects reduced affinity of Dil to its binding pocket and not an allosteric modulation.

Table 3

Midpoints and slope factors of the activation and inactivation curves.

Mutation	$V_{0.5,act}$, mV	k_{act} , mV	$V_{0.5,inact}$, mV	k_{inact} , mV
WT	-6.5 ± 0.7	5.4 ± 0.9	-42.8 ± 0.8	6.6 ± 0.7
T1143A	-5.7 ± 0.7	6.6 ± 0.6	-43.7 ± 0.7	7.5 ± 0.7
T1143C	2.4 ± 0.7	7.6 ± 0.7	-19.3 ± 0.9	10.5 ± 1.0
T1143E	-8.3 ± 0.7	5.6 ± 0.7	-21.5 ± 0.8	7.3 ± 0.7
T1143V	-1.0 ± 0.7	9.5 ± 0.7	-26.2 ± 0.9	13 ± 0.8
T1143L	-24.1 ± 0.7	8.9 ± 0.6	-25.7 ± 1.3	12.6 ± 1.1
T1143N	-6.7 ± 0.7	7.6 ± 0.7	-22.5 ± 1.0	12.9 ± 0.8
T1143S	-9.4 ± 1.14	4.6 ± 0.5	-34.4 ± 0.9	10.7 ± 0.9
T1143Y	-26.1 ± 0.8	6.0 ± 0.7	-42.4 ± 1.3	11.4 ± 1.1

3.4.3 Other substitutions of T1143 affect channel inactivation.

In order to establish a link between amino acid properties and channel block we substituted T1143 by residues with different physicochemical properties, including for example different hydrogen bonding capabilities, size and polarity. All mutations (except the above mentioned alanine) shifted the inactivation curve to more depolarised voltages. Reduced inactivation during a test pulse may thus have affected channel block. Hence, it can not be excluded that some of the observed reduction in use-dependent channel inhibition in mutants T1143E/V/C/N/S can be attributed to removal of channel inactivation via an allosteric mechanism and not to reduction of affinity.

This is, however, not the case for T1143A displaying similar kinetics to wild type (Fig. 5). We speculate that T1143 provides a second hydrogen bond (additionally to Y1463), necessary for high-affinity diltiazem block. Docking studies with the T1143A mutant support the hypothesis that T1143 together with Y1463 serve as anchor points for diltiazem via H-bond formation (see Fig. 7A,B). Fig. 11 shows the best binding pose obtained with the T1143A mutant channel.

Mutations T1143S and T1143Y did not restore WT-like behaviour, although these residues possess hydroxyl groups similar to threonine. Apart from the reduction in inactivation both residues have changed side chain sizes compared to the small T1143. The larger size of these residues may prevent a high-affinity fit of Dil into its binding site.

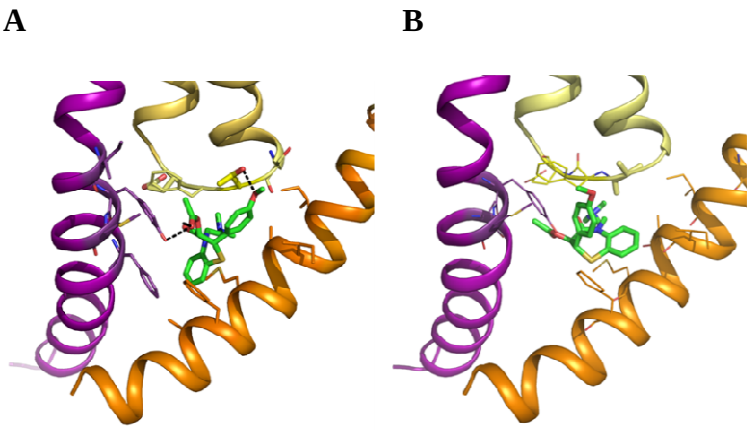

Fig. 11 Docking poses in WT and T1143A models.

A) Hydrogen bonds between diltiazem (green stick representation) and T1143 (yellow sticks) and Y1463 (purple sticks) are shown as black dotted lines. B) In the T1143A mutant no hydrogen bonds are predicted between diltiazem and Cav1.2.

.

REFERENCES

Armstrong CM, Matteson DR: Two distinct populations of calcium channels in a clonal line of pituitary cells. Science 227:65-67 (1985).

Arreola J, Calvo J, Garcia MC, Sanchez JA: Modulation of calcium channels of twitch skeletal muscle fibres of the frog by adrenaline and cyclic adenosine monophosphate. J Physiol 393:307-330 (1987).

Barclay J, Balaguero N, Mione M, Ackerman SL, Letts VA, Brodbeck J, Canti C, Meir A, Page KM, Kusumi K, Perez-Reyes E, Lander ES, Frankel WN, Gardiner RM, Dolphin AC, Rees M: Ducky mouse phenotype of epilepsy and ataxia is associated with mutations in the cacna2d2 gene and decreased calcium channel current in cerebellar purkinje cells. J Neurosci 21:6095-6104 (2001).

Benitah JP, Gomez AM, Fauconnier J, Kerfant BG, Perrier E, Vassort G, Richard S: Voltage-gated ca2+ currents in the human pathophysiologic heart: A review. Basic Res Cardiol 97 Suppl 1:I11-18 (2002).

Berjukow S, Gapp F, Aczel S, Sinnegger MJ, Mitterdorfer J, Glossmann H, Hering S: Sequence differences between alpha1c and alpha1s ca2+ channel subunits reveal structural determinants of a guarded and modulated benzothiazepine receptor. J Biol Chem 274:6154-6160 (1999).

Berjukow S, Marksteiner R, Gapp F, Sinnegger MJ, Hering S: Molecular mechanism of calcium channel block by isradipine. Role of a drug-induced inactivated channel conformation. J Biol Chem 275:22114-22120 (2000).

Beyl S, Timin EN, Hohaus A, Stary A, Kudrnac M, Guy RH, Hering S: Probing the architecture of an l-type calcium channel with a charged phenylalkylamine: Evidence for a widely open pore and drug trapping. J Biol Chem 282:3864-3870 (2007).

Bezanilla F: Voltage sensor movements. J Gen Physiol 120:465-473 (2002).

Bichet D, Cornet V, Geib S, Carlier E, Volsen S, Hoshi T, Mori Y, De Waard M: The i-ii loop of the ca2+ channel alpha1 subunit contains an endoplasmic reticulum retention signal antagonized by the beta subunit. Neuron 25:177-190 (2000).

Birnbaumer L, Qin N, Olcese R, Tareilus E, Platano D, Costantin J, Stefani E: Structures and functions of calcium channel beta subunits. J Bioenerg Biomembr 30:357-375 (1998).

Bodi I, Mikala G, Koch SE, Akhter SA, Schwartz A: The l-type calcium channel in the heart: The beat goes on. J Clin Invest 115:3306-3317 (2005).

Borsotto M, Barhanin J, Fosset M, Lazdunski M: The 1,4-dihydropyridine receptor associated with the skeletal muscle voltage-dependent ca2+ channel. Purification and subunit composition. J Biol Chem 260:14255-14263 (1985).

Brice NL, Berrow NS, Campbell V, Page KM, Brickley K, Tedder I, Dolphin AC: Importance of the different beta subunits in the membrane expression of the alpha1a and alpha2 calcium

channel subunits: Studies using a depolarization-sensitive alpha1a antibody. Eur J Neurosci 9:749-759 (1997).

Bruhova I, Zhorov BS: A homology model of the pore domain of a voltage-gated calcium channel is consistent with available scam data. J Gen Physiol 135:261-274.

Bruhova I, Tikhonov DB, Zhorov BS: Access and binding of local anesthetics in the closed sodium channel. Mol Pharmacol 74:1033-1045 (2008).

Cahalan MD, Wulff H, Chandy KG: Molecular properties and physiological roles of ion channels in the immune system. J Clin Immunol 21:235-252 (2001).

Canti C, Bogdanov Y, Dolphin AC: Interaction between g proteins and accessory subunits in the regulation of 1b calcium channels in xenopus oocytes. J Physiol 527 Pt 3:419-432 (2000).

Canti C, Dolphin AC: Cavbeta subunit-mediated up-regulation of cav2.2 currents triggered by d2 dopamine receptor activation. Neuropharmacology 45:814-827 (2003).

Canti C, Nieto-Rostro M, Foucault I, Heblich F, Wratten J, Richards MW, Hendrich J, Douglas L, Page KM, Davies A, Dolphin AC: The metal-ion-dependent adhesion site in the von willebrand factor-a domain of alpha2delta subunits is key to trafficking voltage-gated ca2+ channels. Proc Natl Acad Sci U S A 102:11230-11235 (2005).

Carafoli E, Santella L, Branca D, Brini M: Generation, control, and processing of cellular calcium signals. Crit Rev Biochem Mol Biol 36:107-260 (2001).

Catterall WA: Structure and regulation of voltage-gated ca2+ channels. Annu Rev Cell Dev Biol 16:521-555 (2000).

Cens T, Restituito S, Galas S, Charnet P: Voltage and calcium use the same molecular determinants to inactivate calcium channels. J Biol Chem 274:5483-5490 (1999).

Chien AJ, Carr KM, Shirokov RE, Rios E, Hosey MM: Identification of palmitoylation sites within the l-type calcium channel beta2a subunit and effects on channel function. J Biol Chem 271:26465-26468 (1996).

Cole RL, Lechner SM, Williams ME, Prodanovich P, Bleicher L, Varney MA, Gu G: Differential distribution of voltage-gated calcium channel alpha-2 delta (alpha2delta) subunit mrna-containing cells in the rat central nervous system and the dorsal root ganglia. J Comp Neurol 491:246-269 (2005).

Colecraft HM, Alseikhan B, Takahashi SX, Chaudhuri D, Mittman S, Yegnasubramanian V, Alvania RS, Johns DC, Marban E, Yue DT: Novel functional properties of ca(2+) channel beta subunits revealed by their expression in adult rat heart cells. J Physiol 541:435-452 (2002).

Corelli F, Manetti F, Tafi A, Campiani G, Nacci V, Botta M: Diltiazem-like calcium entry blockers: A hypothesis of the receptor-binding site based on a comparative molecular field analysis model. J Med Chem 40:125-131 (1997).

Curtis BM, Catterall WA: Purification of the calcium antagonist receptor of the voltage-sensitive calcium channel from skeletal muscle transverse tubules. Biochemistry 23:2113-2118 (1984).

Curtis BM, Catterall WA: Phosphorylation of the calcium antagonist receptor of the voltage-sensitive calcium channel by camp-dependent protein kinase. Proc Natl Acad Sci U S A 82:2528-2532 (1985).

Das J, Floyd DM, Kimball SD, Duff KJ, Vu TC, Lago MW, Moquin RV, Lee VG, Gougoutas JZ, Malley MF, et al.: Benzazepinone calcium channel blockers. 3. Synthesis and structure-activity studies of 3-alkylbenzazepinones. J Med Chem 35:773-780 (1992).

Davies A, Douglas L, Hendrich J, Wratten J, Tran Van Minh A, Foucault I, Koch D, Pratt WS, Saibil HR, Dolphin AC: The calcium channel alpha2delta-2 subunit partitions with cav2.1 into lipid rafts in cerebellum: Implications for localization and function. J Neurosci 26:8748-8757 (2006).

De Jongh KS, Warner C, Catterall WA: Subunits of purified calcium channels. Alpha 2 and delta are encoded by the same gene. J Biol Chem 265:14738-14741 (1990).

de Waard D, Rooijers T: An experimental study to evaluate the effectiveness of different methods and intensities of law enforcement on driving speed on motorways. Accid Anal Prev 26:751-765 (1994).

Dilmac N, Hilliard N, Hockerman GH: Molecular determinants of ca2+ potentiation of diltiazem block and ca2+-dependent inactivation in the pore region of cav1.2. Mol Pharmacol 64:491-501 (2003).

Dilmac N, Hilliard N, Hockerman GH: Molecular determinants of frequency dependence and ca2+ potentiation of verapamil block in the pore region of cav1.2. Mol Pharmacol 66:1236-1247 (2004).

Dolphin AC: Beta subunits of voltage-gated calcium channels. J Bioenerg Biomembr 35:599-620 (2003).

Ellis SB, Williams ME, Ways NR, Brenner R, Sharp AH, Leung AT, Campbell KP, McKenna E, Koch WJ, Hui A, et al.: Sequence and expression of mrnas encoding the alpha 1 and alpha 2 subunits of a dhp-sensitive calcium channel. Science 241:1661-1664 (1988).

Fatt P, Katz B: The electrical properties of crustacean muscle fibres. J Physiol 120:171-204 (1953).

Fleig A, Penner R: Silent calcium channels generate excessive tail currents and facilitation of calcium currents in rat skeletal myoballs. J Physiol 494 (Pt 1):141-153 (1996).

Flockerzi V, Oeken HJ, Hofmann F, Pelzer D, Cavalie A, Trautwein W: Purified dihydropyridine-binding site from skeletal muscle t-tubules is a functional calcium channel. Nature 323:66-68 (1986).

Floyd DM, Kimball SD, Krapcho J, Das J, Turk CF, Moquin RV, Lago MW, Duff KJ, Lee VG, White RE, et al.: Benzazepinone calcium channel blockers. 2. Structure-activity and drug

metabolism studies leading to potent antihypertensive agents. Comparison with benzothiazepinones. J Med Chem 35:756-772 (1992).

Foell JD, Balijepalli RC, Delisle BP, Yunker AM, Robia SL, Walker JW, McEnery MW, January CT, Kamp TJ: Molecular heterogeneity of calcium channel beta-subunits in canine and human heart: Evidence for differential subcellular localization. Physiol Genomics 17:183-200 (2004).

Gao B, Sekido Y, Maximov A, Saad M, Forgacs E, Latif F, Wei MH, Lerman M, Lee JH, Perez-Reyes E, Bezprozvanny I, Minna JD: Functional properties of a new voltage-dependent calcium channel alpha(2)delta auxiliary subunit gene (cacna2d2). J Biol Chem 275:12237-12242 (2000).

Grabner M, Dirksen RT, Beam KG: Tagging with green fluorescent protein reveals a distinct subcellular distribution of l-type and non-l-type ca2+ channels expressed in dysgenic myotubes. Proc Natl Acad Sci U S A 95:1903-1908 (1998).

Gregg RG, Messing A, Strube C, Beurg M, Moss R, Behan M, Sukhareva M, Haynes S, Powell JA, Coronado R, Powers PA: Absence of the beta subunit (cchb1) of the skeletal muscle dihydropyridine receptor alters expression of the alpha 1 subunit and eliminates excitation-contraction coupling. Proc Natl Acad Sci U S A 93:13961-13966 (1996).

Hamill OP, Marty A, Neher E, Sakmann B, Sigworth FJ: Improved patch-clamp techniques for high-resolution current recording from cells and cell-free membrane patches. Pflugers Arch 391:85-100 (1981).

Hering S, Aczel S, Grabner M, Doring F, Berjukow S, Mitterdorfer J, Sinnegger MJ, Striessnig J, Degtiar VE, Wang Z, Glossmann H: Transfer of high sensitivity for benzothiazepines from l-type to class a (bi) calcium channels. J Biol Chem 271:24471-24475 (1996).

Hering S, Aczel S, Kraus RL, Berjukow S, Striessnig J, Timin EN: Molecular mechanism of use-dependent calcium channel block by phenylalkylamines: Role of inactivation. Proc Natl Acad Sci U S A 94:13323-13328 (1997).

Hering S, Berjukow S, Aczel S, Timin EN: Ca2+ channel block and inactivation: Common molecular determinants. Trends Pharmacol Sci 19:439-443 (1998).

Hering S: Beta-subunits: Fine tuning of ca(2+) channel block. Trends Pharmacol Sci 23:509-513 (2002).

Herlitze S, Hockerman GH, Scheuer T, Catterall WA: Molecular determinants of inactivation and g protein modulation in the intracellular loop connecting domains i and ii of the calcium channel alpha1a subunit. Proc Natl Acad Sci U S A 94:1512-1516 (1997).

Hockerman GH, Johnson BD, Scheuer T, Catterall WA: Molecular determinants of high affinity phenylalkylamine block of l-type calcium channels. J Biol Chem 270:22119-22122 (1995).

Hockerman GH, Johnson BD, Abbott MR, Scheuer T, Catterall WA: Molecular determinants of high affinity phenylalkylamine block of l-type calcium channels in transmembrane segment iiis6 and the pore region of the alpha1 subunit. J Biol Chem 272:18759-18765 (1997).

Hockerman GH, Dilmac N, Scheuer T, Catterall WA: Molecular determinants of diltiazem block in domains iiis6 and ivs6 of l-type ca(2+) channels. Mol Pharmacol 58:1264-1270 (2000).

Hosey MM, Barhanin J, Schmid A, Vandaele S, Ptasienski J, O'Callahan C, Cooper C, Lazdunski M: Photoaffinity labelling and phosphorylation of a 165 kilodalton peptide associated with dihydropyridine and phenylalkylamine-sensitive calcium channels. Biochem Biophys Res Commun 147:1137-1145 (1987).

Hymel L, Striessnig J, Glossmann H, Schindler H: Purified skeletal muscle 1,4-dihydropyridine receptor forms phosphorylation-dependent oligomeric calcium channels in planar bilayers. Proc Natl Acad Sci U S A 85:4290-4294 (1988).

Ivanov SV, Ward JM, Tessarollo L, McAreavey D, Sachdev V, Fananapazir L, Banks MK, Morris N, Djurickovic D, Devor-Henneman DE, Wei MH, Alvord GW, Gao B, Richardson JA, Minna JD, Rogawski MA, Lerman MI: Cerebellar ataxia, seizures, premature death, and cardiac abnormalities in mice with targeted disruption of the cacna2d2 gene. Am J Pathol 165:1007-1018 (2004).

Jahn H, Nastainczyk W, Rohrkasten A, Schneider T, Hofmann F: Site-specific phosphorylation of the purified receptor for calcium-channel blockers by camp- and cgmp-dependent protein kinases, protein kinase c, calmodulin-dependent protein kinase ii and casein kinase ii. Eur J Biochem 178:535-542 (1988).

Jay SD, Sharp AH, Kahl SD, Vedvick TS, Harpold MM, Campbell KP: Structural characterization of the dihydropyridine-sensitive calcium channel alpha 2-subunit and the associated delta peptides. J Biol Chem 266:3287-3293 (1991).

Jones LP, Wei SK, Yue DT: Mechanism of auxiliary subunit modulation of neuronal alpha1e calcium channels. J Gen Physiol 112:125-143 (1998).

Josephson IR, Varadi G: The beta subunit increases ca2+ currents and gating charge movements of human cardiac l-type ca2+ channels. Biophys J 70:1285-1293 (1996).

Kang MG, Campbell KP: Gamma subunit of voltage-activated calcium channels. J Biol Chem 278:21315-21318 (2003).

Kimball SD, Floyd DM, Das J, Hunt JT, Krapcho J, Rovnyak G, Duff KJ, Lee VG, Moquin RV, Turk CF, et al.: Benzazepinone calcium channel blockers. 4. Structure-activity overview and intracellular binding site. J Med Chem 35:780-793 (1992).

Klockner U, Mikala G, Schwartz A, Varadi G: Molecular studies of the asymmetric pore structure of the human cardiac voltage- dependent ca2+ channel. Conserved residue, glu-1086, regulates proton-dependent ion permeation. J Biol Chem 271:22293-22296 (1996).

Koch SE, Bodi I, Schwartz A, Varadi G: Architecture of ca(2+) channel pore-lining segments revealed by covalent modification of substituted cysteines. J Biol Chem 275:34493-34500 (2000).

Kraus R, Reichl B, Kimball SD, Grabner M, Murphy BJ, Catterall WA, Striessnig J: Identification of benz(othi)azepine-binding regions within l-type calcium channel alpha1 subunits. J Biol Chem 271:20113-20118 (1996).

Kraus RL, Hering S, Grabner M, Ostler D, Striessnig J: Molecular mechanism of diltiazem interaction with l-type ca2+ channels. J Biol Chem 273:27205-27212 (1998).

Lacinova L, Ludwig A, Bosse E, Flockerzi V, Hofmann F: The block of the expressed l-type calcium channel is modulated by the beta 3 subunit. FEBS Lett 373:103-107 (1995).

Lee KS, Tsien RW: Mechanism of calcium channel blockade by verapamil, d600, diltiazem and nitrendipine in single dialysed heart cells. Nature 302:790-794 (1983).

Leung AT, Imagawa T, Campbell KP: Structural characterization of the 1,4-dihydropyridine receptor of the voltage-dependent ca2+ channel from rabbit skeletal muscle. Evidence for two distinct high molecular weight subunits. J Biol Chem 262:7943-7946 (1987).

Li CY, Song YH, Higuera ES, Luo ZD: Spinal dorsal horn calcium channel alpha2delta-1 subunit upregulation contributes to peripheral nerve injury-induced tactile allodynia. J Neurosci 24:8494-8499 (2004).

Li CY, Zhang XL, Matthews EA, Li KW, Kurwa A, Boroujerdi A, Gross J, Gold MS, Dickenson AH, Feng G, Luo ZD: Calcium channel alpha2delta1 subunit mediates spinal hyperexcitability in pain modulation. Pain 125:20-34 (2006).

Luo ZD, Chaplan SR, Higuera ES, Sorkin LS, Stauderman KA, Williams ME, Yaksh TL: Upregulation of dorsal root ganglion (alpha)2(delta) calcium channel subunit and its correlation with allodynia in spinal nerve-injured rats. J Neurosci 21:1868-1875 (2001).

Luo ZD, Calcutt NA, Higuera ES, Valder CR, Song YH, Svensson CI, Myers RR: Injury type-specific calcium channel alpha 2 delta-1 subunit up-regulation in rat neuropathic pain models correlates with antiallodynic effects of gabapentin. J Pharmacol Exp Ther 303:1199-1205 (2002).

Marais E, Klugbauer N, Hofmann F: Calcium channel alpha(2)delta subunits-structure and gabapentin binding. Mol Pharmacol 59:1243-1248 (2001).

Mathias RT, Cohen IS, Oliva C: Limitations of the whole cell patch clamp technique in the control of intracellular concentrations. Biophys J 58:759-770 (1990).

Meier H: The neuropathology of ducky, a neurological mutation of the mouse. A pathological and preliminary histochemical study. Acta Neuropathol 11:15-28 (1968).

Meir A, Dolphin AC: Kinetics and gbetagamma modulation of ca(v)2.2 channels with different auxiliary beta subunits. Pflugers Arch 444:263-275 (2002).

Mikala G, Bahinski A, Yatani A, Tang S, Schwartz A: Differential contribution by conserved glutamate residues to an ion-selectivity site in the l-type ca2+ channel pore. FEBS Lett 335:265-269 (1993).

Motoike HK, Bodi I, Nakayama H, Schwartz A, Varadi G: A region in ivs5 of the human cardiac l-type calcium channel is required for the use-dependent block by phenylalkylamines and benzothiazepines. J Biol Chem 274:9409-9420 (1999).

Murakami M, Yamamura H, Murakami A, Okamura T, Nunoki K, Mitui-Saito M, Muraki K, Hano T, Imaizumi Y, Flockerzi T, Yanagisawa T: Conserved smooth muscle contractility and blood pressure increase in response to high-salt diet in mice lacking the beta3 subunit of the voltage-dependent calcium channel. J Cardiovasc Pharmacol 36 Suppl 2:S69-73 (2000).

Nastainczyk W, Rohrkasten A, Sieber M, Rudolph C, Schachtele C, Marme D, Hofmann F: Phosphorylation of the purified receptor for calcium channel blockers by camp kinase and protein kinase c. Eur J Biochem 169:137-142 (1987).

Neely A, Wei X, Olcese R, Birnbaumer L, Stefani E: Potentiation by the beta subunit of the ratio of the ionic current to the charge movement in the cardiac calcium channel. Science 262:575-578 (1993).

Newton RA, Bingham S, Case PC, Sanger GJ, Lawson SN: Dorsal root ganglion neurons show increased expression of the calcium channel alpha2delta-1 subunit following partial sciatic nerve injury. Brain Res Mol Brain Res 95:1-8 (2001).

Nilius B, Hess P, Lansman JB, Tsien RW: A novel type of cardiac calcium channel in ventricular cells. Nature 316:443-446 (1985).

O'Callahan CM, Ptasienski J, Hosey MM: Phosphorylation of the 165-kda dihydropyridine/phenylalkylamine receptor from skeletal muscle by protein kinase c. J Biol Chem 263:17342-17349 (1988).

Olcese R, Qin N, Schneider T, Neely A, Wei X, Stefani E, Birnbaumer L: The amino terminus of a calcium channel beta subunit sets rates of channel inactivation independently of the subunit's effect on activation. Neuron 13:1433-1438 (1994).

Olcese R, Neely A, Qin N, Wei X, Birnbaumer L, Stefani E: Coupling between charge movement and pore opening in vertebrate neuronal alpha 1e calcium channels. J Physiol 497 (Pt 3):675-686 (1996).

Opatowsky Y, Chomsky-Hecht O, Kang MG, Campbell KP, Hirsch JA: The voltage-dependent calcium channel beta subunit contains two stable interacting domains. J Biol Chem 278:52323-52332 (2003).

Perez-Reyes E: Molecular physiology of low-voltage-activated t-type calcium channels. Physiol Rev 83:117-161 (2003).

Pragnell M, De Waard M, Mori Y, Tanabe T, Snutch TP, Campbell KP: Calcium channel beta-subunit binds to a conserved motif in the i-ii cytoplasmic linker of the alpha 1-subunit. Nature 368:67-70 (1994).

Qin N, Platano D, Olcese R, Costantin JL, Stefani E, Birnbaumer L: Unique regulatory properties of the type 2a ca2+ channel beta subunit caused by palmitoylation. Proc Natl Acad Sci U S A 95:4690-4695 (1998).

Qin N, Yagel S, Momplaisir ML, Codd EE, D'Andrea MR: Molecular cloning and characterization of the human voltage-gated calcium channel alpha(2)delta-4 subunit. Mol Pharmacol 62:485-496 (2002).

Raghib A, Bertaso F, Davies A, Page KM, Meir A, Bogdanov Y, Dolphin AC: Dominant-negative synthesis suppression of voltage-gated calcium channel cav2.2 induced by truncated constructs. J Neurosci 21:8495-8504 (2001).

Reuter H: The dependence of slow inward current in purkinje fibres on the extracellular calcium-concentration. J Physiol 192:479-492 (1967).

Reuter H, Stevens CF, Tsien RW, Yellen G: Properties of single calcium channels in cardiac cell culture. Nature 297:501-504 (1982).

Rohrkasten A, Meyer HE, Nastainczyk W, Sieber M, Hofmann F: Camp-dependent protein kinase rapidly phosphorylates serine- 687 of the skeletal muscle receptor for calcium channel blockers. J Biol Chem 263:15325-15329 (1988).

Rotman EI, De Jongh KS, Florio V, Lai Y, Catterall WA: Specific phosphorylation of a cooh-terminal site on the full-length form of the alpha 1 subunit of the skeletal muscle calcium channel by camp-dependent protein kinase. J Biol Chem 267:16100-16105 (1992).

Rotman EI, Murphy BJ, Catterall WA: Sites of selective camp-dependent phosphorylation of the l-type calcium channel alpha 1 subunit from intact rabbit skeletal muscle myotubes. J Biol Chem 270:16371-16377 (1995).

Ruth P, Rohrkasten A, Biel M, Bosse E, Regulla S, Meyer HE, Flockerzi V, Hofmann F: Primary structure of the beta subunit of the dhp-sensitive calcium channel from skeletal muscle. Science 245:1115-1118 (1989).

Schmid A, Renaud JF, Lazdunski M: Short term and long term effects of beta-adrenergic effectors and cyclic amp on nitrendipine-sensitive voltage-dependent ca2+ channels of skeletal muscle. J Biol Chem 260:13041-13046 (1985).

Sculptoreanu A, Scheuer T, Catterall WA: Voltage-dependent potentiation of l-type ca2+ channels due to phosphorylation by camp-dependent protein kinase. Nature 364:240-243 (1993).

Shabbir W, Beyl S, Timin EN, Schellmann D, Erker T, Hohaus A, Hockerman GH, Hering S: Interaction of diltiazem with an intracellularly accessible binding site on ca(v)1.2. Br J Pharmacol 162:1074-1082.

Sharp AH, Campbell KP: Characterization of the 1,4-dihydropyridine receptor using subunit-specific polyclonal antibodies. Evidence for a 32,000-da subunit. J Biol Chem 264:2816-2825 (1989).

Shistik E, Ivanina T, Puri T, Hosey M, Dascal N: Ca2+ current enhancement by alpha 2/delta and beta subunits in xenopus oocytes: Contribution of changes in channel gating and alpha 1 protein level. J Physiol 489 (Pt 1):55-62 (1995).

Sieber M, Nastainczyk W, Zubor V, Wernet W, Hofmann F: The 165-kda peptide of the purified skeletal muscle dihydropyridine receptor contains the known regulatory sites of the calcium channel. Eur J Biochem 167:117-122 (1987).

Sokolov S, Timin E, Hering S: On the role of ca(2+)- and voltage-dependent inactivation in ca(v)1.2 sensitivity for the phenylalkylamine (-)gallopamil. Circ Res 89:700-708 (2001).

Spaetgens RL, Zamponi GW: Multiple structural domains contribute to voltage-dependent inactivation of rat brain alpha(1e) calcium channels. J Biol Chem 274:22428-22436 (1999).

Stary A, Shafrir Y, Hering S, Wolschann P, Guy HR: Structural model of the ca v 1.2 pore. Channels (Austin) 2:210-215 (2008).

Sutton KG, Martin DJ, Pinnock RD, Lee K, Scott RH: Gabapentin inhibits high-threshold calcium channel currents in cultured rat dorsal root ganglion neurones. Br J Pharmacol 135:257-265 (2002).

Takahashi M, Catterall WA: Dihydropyridine-sensitive calcium channels in cardiac and skeletal muscle membranes: Studies with antibodies against the alpha subunits. Biochemistry 26:5518-5526 (1987).

Takahashi M, Narisawa T, Masuda T, Nagasawa O, Suzuki K, Yoshioka H, Koyama H: [inhibition of the growth of a murine transplantable tumor, colon 26, by the prostaglandin synthetase inhibitor, indomethacin]. Gan To Kagaku Ryoho 14:2334-2340 (1987a).

Takahashi M, Seagar MJ, Jones JF, Reber BF, Catterall WA: Subunit structure of dihydropyridine-sensitive calcium channels from skeletal muscle. Proc Natl Acad Sci U S A 84:5478-5482 (1987b).

Takahashi SX, Mittman S, Colecraft HM: Distinctive modulatory effects of five human auxiliary beta2 subunit splice variants on l-type calcium channel gating. Biophys J 84:3007-3021 (2003).

Tanabe T, Takeshima H, Mikami A, Flockerzi V, Takahashi H, Kangawa K, Kojima M, Matsuo H, Hirose T, Numa S: Primary structure of the receptor for calcium channel blockers from skeletal muscle. Nature 328:313-318 (1987).

Tikhonov DB, Zhorov BS: Molecular modeling of benzothiazepine binding in the l-type calcium channel. J Biol Chem 283:17594-17604 (2008).

Triggle DJ: Drug targets in the voltage-gated calcium channel family: Why some are and some are not. Assay Drug Dev Technol 1:719-733 (2003).

Triggle DJ: L-type calcium channels. Curr Pharm Des 12:443-457 (2006).

Triggle DJ: Calcium channel antagonists: Clinical uses--past, present and future. Biochem Pharmacol 74:1-9 (2007).

Uehara A, Hume JR: Interactions of organic calcium channel antagonists with calcium channels in single frog atrial cells. J Gen Physiol 85:621-647 (1985).

Vaghy PL, Striessnig J, Miwa K, Knaus HG, Itagaki K, McKenna E, Glossmann H, Schwartz A: Identification of a novel 1,4-dihydropyridine- and phenylalkylamine-binding polypeptide in calcium channel preparations. J Biol Chem 262:14337-14342 (1987).

Viard P, Butcher AJ, Halet G, Davies A, Nurnberg B, Heblich F, Dolphin AC: Pi3k promotes voltage-dependent calcium channel trafficking to the plasma membrane. Nat Neurosci 7:939-946 (2004).

Wang H, Sun H, Della Penna K, Benz RJ, Xu J, Gerhold DL, Holder DJ, Koblan KS: Chronic neuropathic pain is accompanied by global changes in gene expression and shares pathobiology with neurodegenerative diseases. Neuroscience 114:529-546 (2002).

Williams ME, Brust PF, Feldman DH, Patthi S, Simerson S, Maroufi A, McCue AF, Velicelebi G, Ellis SB, Harpold MM: Structure and functional expression of an omega-conotoxin-sensitive human n-type calcium channel. Science 257:389-395 (1992).

Yamaguchi H, Hara M, Strobeck M, Fukasawa K, Schwartz A, Varadi G: Multiple modulation pathways of calcium channel activity by a beta subunit. Direct evidence of beta subunit participation in membrane trafficking of the alpha1c subunit. J Biol Chem 273:19348-19356 (1998).

Yokoyama CT, Myers SJ, Fu J, Mockus SM, Scheuer T, Catterall WA: Mechanism of snare protein binding and regulation of cav2 channels by phosphorylation of the synaptic protein interaction site. Mol Cell Neurosci 28:1-17 (2005).

Zamponi GW, Soong TW, Bourinet E, Snutch TP: Beta subunit coexpression and the alpha1 subunit domain i-ii linker affect piperidine block of neuronal calcium channels. J Neurosci 16:2430-2443 (1996).

Zhang HL, Schoenberg SO, Resnick LM, Prince MR: Diagnosis of renal artery stenosis: Combining gadolinimum-enhanced three-dimensional magnetic resonance angiography with functional magnetic resonance pulse sequences. Am J Hypertens 16:1079-1082 (2003).

Zhang JF, Ellinor PT, Aldrich RW, Tsien RW: Molecular determinants of voltage-dependent inactivation in calcium channels. Nature 372:97-100 (1994).

4 SUMMARY OF THE THESIS

Quaternary derivative d-cis-diltiazem inhibited Ca(V)1.2 when applied to the intracellular side of the membrane in a use-dependent manner and induced only a low level of tonic (non-use-dependent) block when applied to the extracellular side of the membrane. The latter finding suggests an intracellular access path of Dil to its binding site (Shabbier et al. BJP 2011). Data of my second study demonstrate: i) strong reduction of use-dependent and resting state I_{Ba} inhibition by Dil and qDil when a threonine in the selectivity filter of domain III (T1143) is mutated to alanine. The alanine mutation (T1143A) had no effect on current kinetics suggesting that T1143 forms a binding determinant for Dil and qDil).

5 ACKNOWLEDGEMENTS

It is a pleasure to thank those who made this thesis possible. I would like to thank university of Vienna, IK Kolleg (MDT), for financially supporting my work. I owe my deepest gratitude to my Mentor, Prof. Dr. Steffen Hering, whose encouragement, supervision and support from the preliminary to the concluding level enabled me to develop an understanding of the subject. I would like to thank Dr. Eugen Timin for his generosity and very elaborative discussions. Thanks to Dr. Stanislav Beyl for helping me to understand Electrophysiology and data analysis. Words are lacking to thank my colleague Dr. Annette Hohaus head of the molecular biology unit for her patience and understanding and I am also thankful to Christine Weiz (Technician Mol .Bio). I would like to thank Dr. Anna Weinzinger who performed the molecular modelling studies (Figs. 1, 7, 10, 11) and for suggesting T1143 as a potential binding determinant for Dil. I am deeply thankful to Mag. Katrin Depil, who never hesitates to go extra mileage with me.

Finally, I would also like to thank my family and parents for their necessary support and encouragement.

6 C.V

Waheed Shabbir

CURRICULUM VITAE

PERSONAL DATA

Date and place of Birth May 17th, 1972, Pakistan

EDUCATION

1980-1989	Matriculation in science, Laboratory high school, Faisal abad, Pakistan
1989-1994	Fsc. Pre medical, Government college Faisal abad, Pakistan
1994-2000	Bsc.(Hons) University of Agriculature , Faisal abad, Pakistan
2000-2005	Student of university of Applied life sciences Vienna, Austria
2005-2007	Master of molecular bio-Engineering, university of technology, Graz, Austria
2007	PhD student

RESEARCH INTERESTS

Molecular biology of ion channels, Electrophysiology

PUBLICATIONS

1. Shabbir W, Beyl S, Timin E, Schellmann D, Erker T, Hohaus A, Hockerman G, Hering S. Interaction of diltiazem with an intracellularly accessible binding site on Ca(V) 1.2. Br J Pharmacol. 2010 Oct 26. doi: 10.1111/j.1476-5381.2010.01091

2. Brünner-Kubath C, Shabbir W, Saferding V, Wagner R, Singer CF, Valent P, Berger W, Marian B, Zielinski CC, Grusch M, Grunt TW

Breast Cancer Res Treat. 2010 Nov 3. PMID: 21046231

3. Beyl S, Depil K, Hohaus A, Stary-Weinzinger A, Timin E, Shabbir W, Kudrnac M, Hering S.

Physicochemical properties of pore residues predict activation gating of Ca(V)1.2: A correlation mutation analysis. PMID: 20924598 Pflugers Arch. 2010 Oct 7.

PATENT

Shabbir,W., Grunt,T.: Biomarkers for EGFR/HER/ERBB drug efficacy.

US Provisonal Patent AM103145L1 filed August, 2009